AFRL-IF-RS-TR-2005-229
Final Technical Report
June 2005

OPTIMIZING THE IMMUNO-SURFACE CHARACTERISTICS FOR BIO-SENSORS AND FILTERS THROUGH MODELING AND EXPERIMENTS

Purdue University

Sponsored by
Defense Advanced Research Projects Agency
DARPA Order No. E117

AIR FORCE RESEARCH LABORATORY
INFORMATION DIRECTORATE
ROME RESEARCH SITE
ROME, NEW YORK

STINFO FINAL REPORT

This report has been reviewed by the Air Force Research Laboratory, Information Directorate, Public Affairs Office (IFOIPA) and is releasable to the National Technical Information Service (NTIS). At NTIS it will be releasable to the general public, including foreign nations.

AFRL-IF-RS-TR-2005-229 has been reviewed and is approved for publication

APPROVED: /s/

DANIEL J. BURNS
Project Engineer

FOR THE DIRECTOR: /s/

JAMES A. COLLINS, Acting Chief
Advanced Computing Division
Information Directorate

REPORT DOCUMENTATION PAGE

Form Approved
OMB No. 074-0188

1. AGENCY USE ONLY (Leave blank)	2. REPORT DATE	3. REPORT TYPE AND DATES COVERED
	JUNE 2005	Final Jun 01 – Nov 04

4. TITLE AND SUBTITLE
OPTIMIZING THE IMMUNO-SURFACE CHARACTERISTICS FOR BIO-SENSORS AND FILTERS THROUGH MODELING AND EXPERIMENTS

5. FUNDING NUMBERS
C - F30602-01-2-0539
PE - 61101E
PR -E117
TA - 00
WU - 68

6. AUTHOR(S)
Ann E. Rundell,
Harm HogenEsch,
Thomas J. Webster

7. PERFORMING ORGANIZATION NAME(S) AND ADDRESS(ES)
Purdue University
Department of Biomedical Engineering
West Lafayette Indiana 47907-2022

8. PERFORMING ORGANIZATION REPORT NUMBER
N/A

9. SPONSORING / MONITORING AGENCY NAME(S) AND ADDRESS(ES)
Defense Advanced Research Projects Agency
3701 North Fairfax Drive
Arlington Virginia 22203-1714

AFRL/IFTC
26 Electronic Parkway
Rome New York 13441-4514

10. SPONSORING / MONITORING AGENCY REPORT NUMBER
AFRL-IF-RS-TR-2005-229

11. SUPPLEMENTARY NOTES
AFRL Project Engineer: Daniel J. Burns/IFTC/(315) 330-2335/ Daniel.Burns@rl.af.mil

12a. DISTRIBUTION / AVAILABILITY STATEMENT
APPROVED FOR PUBLIC RELEASE; DISTRIBUTION UNLIMITED.

12b. DISTRIBUTION CODE

13. ABSTRACT *(Maximum 200 Words)*
The scope of this work integrated experimental exploration with model development, and optimization studies for determining the best configuration and composition of immuno-surfaces for biosensors as inspired by the B-cell membrane. One objective of this work was to determine alteration in antigen capture on immuno-surfaces as a function of antibody density and functionality achieved by different protein immobilization methods. Another was to generate a model that reflects multivalent antigen binding dynamics to immobilized antibodies and incorporates the effective far-field antibody surface density, the local antibody surface density once the antibody is bound, and the flexibility and functional range of motion of the immobilized antibodies. The study also designed, synthesized, and evaluated the influence of surface roughness and energetics on immunoassay functionality. Finally, two mathematical models were created to quantitatively evaluate the effects of antibody and epitope diffusion on antigen capture.

14. SUBJECT TERMS
Immunosurface, Antigen, Binding, Dynamics, Model, Characterization, Evaluation, Simulation, B-Cell, Membrane Flexibility

15. NUMBER OF PAGES
58

16. PRICE CODE

17. SECURITY CLASSIFICATION OF REPORT	18. SECURITY CLASSIFICATION OF THIS PAGE	19. SECURITY CLASSIFICATION OF ABSTRACT	20. LIMITATION OF ABSTRACT
UNCLASSIFIED	UNCLASSIFIED	UNCLASSIFIED	UL

Table of Contents

List of Figures

List of Tables

Summary

Project Goals:

The scope of this work integrated experimental exploration with model development, validation, and optimization studies for determining the best configuration and composition of immuno-surfaces as inspired by the B-cell membrane. Specifically, the influence of membrane flexibility and properties on the interaction between membrane-fixed antibodies and specific antigens were investigated and modeled.

Major Accomplishments

Experimental Aspects

- Compared the functionality of different methods for immobilization of antibodies
  - Adsorbed, aminophase, heterobifunctional crosslinkers (GMBS, BMPS, EMCS)
  - GMBS attaches the most antibodies
  - ProteinA antibody orientation using GMBS or adsorbed methods does better than randomly attached antibodies
- Characterized immobilized Protein A surfaces using an atomic force microscope
  - Aminophase surfaces were punctate while adsorbed and GMBS surfaces seemed to completely cover the glass surface
    - May partially explain the larger non-specific binding by aminophase
  - The GMBS surfaces had the most surface roughness while the adsorbed surfaces were the least
- Compared functionality of immuno-surfaces constructed with different degrees of surface roughness
  - Characterized different constructions in terms of their surface roughness (as measured by the AFM) and their surface energies (via contact angles)
  - Observed enhanced functionality of immuno-surfaces with increased degrees of surface roughness
  - Observed enhanced functionality of immuno-surfaces with increased degrees of hydrophilicity

Analytical Aspects

- Explored a refined sequential binding model for potential means to enhance antigen capture through immuno-surface design
  - Use high affinity antibodies with low dissociation rates
  - There exists an optimal antibody surface density which is independent of the antigen characteristics, this density is roughly $1.5e^{-10}$ moles/dm^2
  - Antibody extension, surface roughness, membrane flexibility have the potential to enhance antigen capture (enhancement capability is a function of IgG affinity)
- Incorporated both antibody and antigen epitope diffusion on membranes
  - Found for antigen with numerous epitopes, the diffusion of the antibodies is more important than the diffusion of the antigen epitopes on the effectiveness of the antigen capture

Recommended Future Research Directions

- Utilize customized crosslinker for covalently immobilizing antibodies to surfaces
- Compare performance of immuno-surfaces with varying degrees of surface roughness with similar surface chemistries
- Refine mathematical model to incorporate more fundamental principles from physics and chemistry at the intermolecular and surface force level

1.0 Impact of Antibody Immobilization Techniques on Immuno-surface Functionality

Several groups have compared various methods of antibody attachment methods for the development of immuno-surfaces for biosensors including simple physiochemical adsorption, Langmuir-Blodgett methods, and covalent attachment (Ahluwalia *et al*., 1991; Bhatia *et al*., 1993; Shriver-Lake *et al*., 1997). In the past, several immuno-sensors have relied on adsorption to immobilize antibodies onto a surface thus allowing for specific detection and binding of antigen through the antibody-antigen interaction. Adsorbed surfaces in solution are more susceptible to instability as desorption may occur due to the reversible nature of non-covalent attachment. Comparatively, covalent linkages limit desorption of proteins through increased bond strength. In addition, as proteins adsorb, protein unfolding occurs leading to protein inactivity through modification or reduction of essential binding sites.

Covalent binding of proteins to surfaces has been investigated as an alternative to adsorption due to increased stability and control of protein binding site availability. One major drawback to covalent attachment is that these methods can lead to a loss of protein activity. For example, several chemical crosslinkers that immobilize proteins induce crosslinking of the protein itself, which limits the availability of binding sites for antigen capture. This realization has lead to the development of several protein immobilization techniques that bind a specific location on the protein thus limiting crosslinking and inactivity (Zull *et al*., 1994).

The work presented here has focused on comparing immuno-surface antibody density and functionality for three antibody immobilization techniques. Each of these techniques utilize a different method of attaching protein to glass either covalently linking to protein amine or carboxyl groups, or through adsorption. These different immobilization techniques may result in surfaces with different capacities for specific antibody capture due differences in the surface chemistry or antibody attachment. Adsorption was specifically chosen because it is widely used in biosensor production due to its simplicity and cost-effectiveness. The adsorption technique investigated primarily relies on non-specific electrostatic and hydrophobic interactions to immobilize protein. The aminophase technique was investigated primarily because it has been used to immobilize several biological molecules including peptide sequences to promote cell-adhesion (Kouvroukoglou *et al*., 2000). The aminophase treatment covalently binds proteins through carboxyl or carbohydrate groups to amine groups on a silanized surface through an EDC (1-Ethyl-3-(3-dimethylaminopropyl)carbodiimide) reaction. It has been shown previously that surface chemistries which target carbohydrates allow for greater antibody functionality due to the comparatively larger presence of carbohydrates in the Fc, or constant region of the antibody (Shriver-Lake *et al.,* 1997). By covalently linking the Fc region, the Fab regions are free to function by binding antigen. Lastly, GMBS and other succinimide esters have also been utilized to immobilize biological molecules onto several surfaces designed for biosensor use (Bhatia *et al*., 1993; Shriver-Lake *et al*., 1997). The GMBS procedure covalently binds proteins through amine groups to immobilized silanes through a heterobifunctional crosslinker (GMBS). This crosslinker serves as a tether between protein amine groups and the surface-immobilized silane groups. GMBS has been found to successfully immobilize antibodies to immuno-surfaces and retain a moderate amount of function (Shriver-Lake *et al*., 1997).

In addition to the immobilization techniques described above, the role of protein A in these attachment schemes was investigated. One of the most common methods of immobilizing antibodies at the Fc region is through the utilization of protein A (Anderson *et al*., 1997; Babacan

et al., 2000; König and Grätzel, 1994; Lu *et al*., 1996). Oriented, functional antibodies are achieved by utilizing protein A, which binds IgG_{2a} in its constant heavy chain region (Fc) leaving the variable light chain regions (Fab) available for binding to antigen epitopes (Turkova, 1999). Protein A is a 64 kDa bacterial surface protein extracted from the bacterium *Staphylococcus aureus*. König and Grätzel (1994) have shown that immobilization methods including protein A give the best results in terms of biosensor sensitivity, stability, and reusability, while Lu *et al.* (1996) have shown 2-8 times higher antigen-binding capacity when oriented coupling techniques such as protein A are used. Babacan *et al.* (2000) and Anderson *et al.* (1997) have presented similar results.

Overall, the objective of this work was to determine alterations in antigen capture on immuno-surfaces as a function of antibody density and functionality achieved by different protein immobilization methods. Adsorbed, aminosilane, and GMBS methods were specifically investigated for their ability to create functional immuno-surfaces with and without protein A. See Figure 1. For the Materials and Methods please see R. Danczyk, et al. 2003

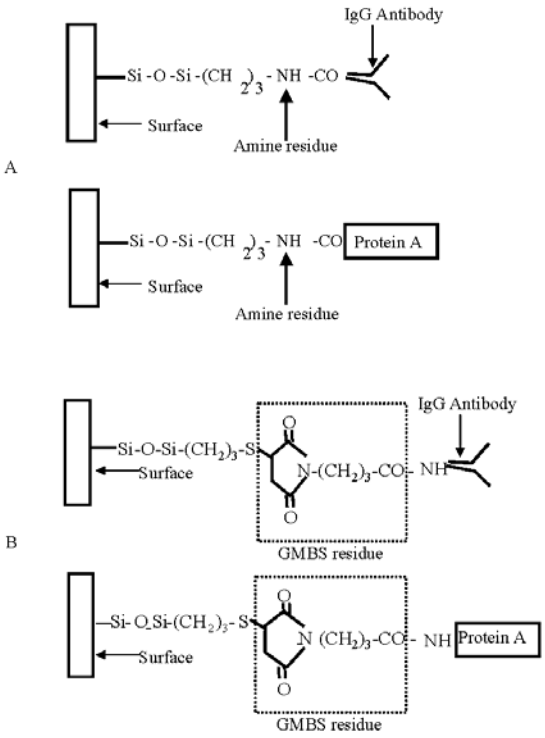

Figure 1: Illustration of aminophase (A) and GMBS (B) attachment methods showing attachment of protein A and IgG antibody through carbohydrate (A) and amine (B) groups present in the protein, respectively. The aminophase method utilizes an EDC reaction to link amine groups on the surface to carbohydrates/carboxyls present in the protein. The GMBS method serves as a heterobifunctional crosslinker to immobilize the protein via one of its amine groups to the surface.

Results and Discussion
1.1 Surface Analysis

1.1.1 Antibody Surface Density – The results shown in Table I show the amount of antibody immobilized using the described methods with and without protein A. Surprisingly, this technique indicated the amount of antibody immobilized on the protein A immuno-surfaces is less than the amount of antibody immobilized directly onto the surface for each immobilization technique. Protein A has been known to bind approximately 2-5 antibodies per protein A molecule (Turkova, 1999); however, this was not demonstrated by the data. It is hypothesized that protein A conformation changes occurring at the immuno-surface limited the number of antibody-binding sites available. Additionally, steric hindrance may have limited binding between protein A and the antibodies. Even as the GMBS method increased the amount of protein A present on the surfaces, a significant increase in the amount of antibody was not observed when compared to adsorbed and aminophase surfaces (see Table I).

Table I: MicroBCA™ protein assay results in mean μg/cm^2 +/- SEM, n=3.

	Adsorbed	**Aminophase**	**GMBS**
PA	2.08 +/- 0.18	2.26 +/- 0.16	*4.97 +/- 0.41
PA+BSA	2.16 +/- 0.11	3.02 +/- 0.32	5.55 +/- 0.50
PA+BSA+IgG	2.24 +/- 0.14	3.04 +/- 0.43	*5.89 +/- 0.20
IgG on PA Surfaces	0.08 +/- 0.03	0.03 +/- 0.20	0.35 +/- 0.06
IgG	2.19 +/- 0.29	2.36 +/- 0.21	*5.18 +/- 0.24
IgG+BSA	2.34 +/- 0.14	2.92 +/- 0.33	*5.59 +/- 0.34

*****Significant increase compared to adsorbed and aminophase surfaces, p-value<0.05.

The highest amount of antibody immobilized onto the immuno-surfaces is achieved using GMBS without protein A (5.18 μg/cm^2). This amount of antibody is considerably greater than the amount achieved by Bhatia *et al.* (1993) of 0.121μg/cm^2 IgG. There are several factors that may have contributed to our increased antibody surface density as compared to previous results. It is hypothesized that the increase in antibody and protein density at the surface is due to the formation of protein aggregates on the surface rather than the formation of an even protein monolayer (Aslam & Dent, 1998). Additionally, the coverslip cleaning treatment used by Bhatia *et al.* was considerably harsher, potentially leading to a lower surface roughness than our prepared samples which will have lower amounts of IgG immobilized. Also, a PBS wash was performed prior to performing the MicroBCA™ assay rather than the standard urea/salt wash to avoid interference of the residual urea and the MicroBCA™ reagents. The PBS wash most likely did not remove as much protein as the urea/salt wash would have, thus leading to an elevated amount of protein present on our surfaces. There was no statistical difference in the amount of antibody immobilized by any method with protein A. In addition, the average amount of BSA immobilized onto each immuno-surface was 0.42 μg/cm^2.

1.1.2 Contact Angle Analysis – The surface hydrophilicity could impact the immuno-surface antigen capture capabilities. Contact angle measurements were used to compare the hydrophilicity of the immuno-surfaces. As seen in Table II, the initial glass surface had a contact angle of 59° prior to treatment. After surfaces were piranha etched (80:20 H2O2/H2SO4), the contact angle of the surface decreased significantly to 33° indicating a change in surface energy since the surface became more hydrophilic upon piranha treatment. Once protein A was bound to the piranha-treated surfaces, and BSA was applied, the contact angle increased to 76°, 60°, and 70° for adsorbed, aminophase, and GMBS treated surfaces, respectively. This significant increase indicated a shift from a hydrophilic surface to a more hydrophobic surface with each final surface treatment. The difference in contact angles between the three surface treatments was statistically significant. In terms of hydrophilicity, the aminophase surface was the most hydrophilic, while the adsorbed surfaces were the least hydrophilic. Contact angles shown here are for protein A + BSA surfaces only. Contact angle measurements were also performed on IgG2aαDNP + BSA and protein A + BSA+ IgG2aαDNP surfaces; however, there was no statistically significant difference between these surfaces and protein A + BSA surfaces based upon ANOVA (data not shown).

Table II: Contact angles for protein A + BSA prepared surfaces in deg., n=3.

	Glass	Piranha Glass	Adsorbed	Aminophase	GMBS
	58	**32**	**75**	**60**	**71**
	60	**34**	**75**	**64**	**70**
	60	**32**	**77**	**56**	**69**
Mean	***59**	**33**	***76**	***,#60**	***,#70**
SEM	**1**	**1**	**1**	**4**	**1**

*Significant increase in contact angle compared to piranha glass surface mean, p-value<0.05.
#Significant decrease in contact angle compared to adsorbed and/or GBMS surface means, p<0.05.

1.1.3 AFM Determination of Protein A Surface Characteristics - Adsorbed, aminophase, and GMBS immobilized protein A surfaces were explored using tapping mode AFM in liquid to determine the spatial distribution of protein A. The following section will describe the observed results. The impact of these results on antigen capture, both non-specific and specific, will be discussed in later sections.

Fig. 2 shows AFM amplitude images of piranha-treated glass and protein A immobilized via aminophase, adsorption, and GMBS procedures on glass. The glass surface prior to protein A immobilization was uniform as expected (image A). Aminophase immobilization of protein A yielded punctate aggregates on the surface as shown in image B. Image C shows a uniform and smooth surface illustrating even coverage of the surface through protein A adsorption at pH 7.4. Image D (GMBS) shows a rough, non-uniform surface without punctate regions present. All images (B-D) were visibly different than glass alone.

To quantify the differences between the surface treatments, the surface roughness and apparent surface area (surface area increase due to Z-direction roughness; in addition to 1 μm^2 surface area sample), was calculated from three height images taken at random locations on a sample of each surface type. The results are shown in Tables 3 and 4. ANOVA determined that

the surface treatments were significantly different from one another. Following ANOVA, Duncan's multiple range tests showed that the adsorbed protein A surface was significantly smoother than the glass and GMBS surfaces (see Table 3). No other increases were determined to be significant. These results support the observation in Fig. 2 that the adsorbed surfaces were smoothest compared to GMBS and glass surfaces as illustrated.

Table 3 also illustrates that surface roughness varied greatly between random locations on GMBS-immobilized protein A surfaces compared to adsorbed- and aminophase-immobilized protein A surfaces. This observation was supported by the fact that the SEM for GMBS surfaces was nearly an order of magnitude greater than that of adsorbed or aminophase SEM values (GMBS, 1.118; adsorbed, 0.121; aminophase, 0.278).

Table 4 illustrates that surface area increased significantly following GMBS treatment when compared to glass, adsorbed, and aminophase protein A surfaces. Additionally, the glass surface exhibited increased surface area compared to adsorbed and aminophase protein A surfaces.

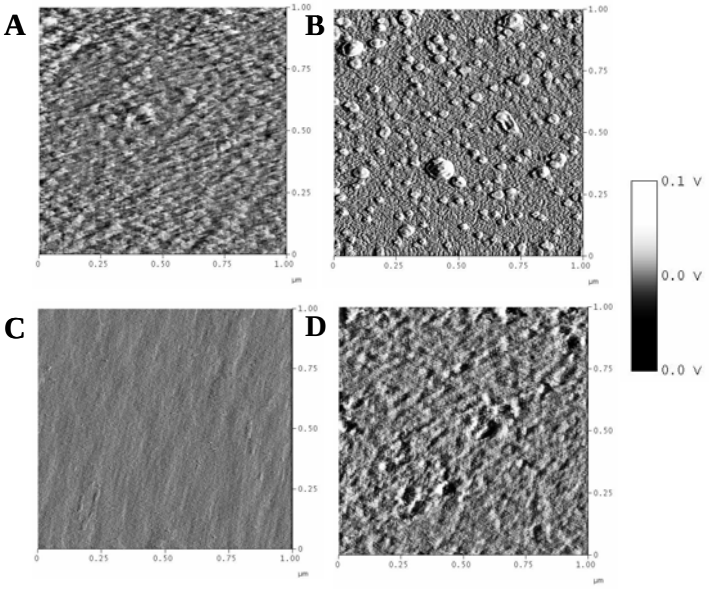

Figure 2: AFM amplitude images of piranha-treated glass (A), aminophase-immobilized protein A (B), adsorbed protein A (C), and GMBS-immobilized protein A (D). Each image is 512 X 512 resolution obtained with a tip velocity of 3.94 µm/sec (1.97 Hz). Amplitude set points: A, 0.8829 V; B, 1.097 V; C, 0.8223 V; D, 0.6814 V.

Table III: Surface roughness (RMS value) of protein A prepared surfaces given in nm, n=3. *Significant increase compared to adsorbed mean, $p<0.05$.

	Glass	**Adsorbed**	**Aminophase**	**GMBS**
	518204	457718	427377	566538
	485211	455435	462030	584481
	520721	400672	434461	617049
Mean	#508045	437942	441289	*589356
SEM	11440	18646	10570	14784

Table IV: Surface area increase due to Z-direction roughness of protein A prepared surfaces given in nm^2, n=3. #Significant increase in surface area compared to adsorbed and aminophase surface area means, $p<0.05$. *Significant increase in surface area compared to glass, aminophase, and adsorbed surface area means, $p<0.05$.

	Glass	Adsorbed	Aminophase	GMBS
	6.052	0.810	3.062	4.223
	2.683	0.849	2.789	5.651
	5.729	1.191	2.126	1.820
Mean	*4.821	0.950	2.659	*3.898
SEM	1.073	0.121	0.278	1.118

1.2 Functionality of Immuno-surfaces

1.2.1 Non-specific Interactions - Antigen capture experiments performed on aminophase-prepared control surfaces (protein A + BSA) showed the highest amount of non-specific binding for both BSA and DNP-BSA MS (Fig. 3). This result led to the hypothesis that aminophase surface hydrophilicity may be increasing the non-specific binding of antigen to the surface. It is possible that charges associated with the hydrophilic aminophase surface are interacting with the charge densities associated with the MS, causing them to bind non-specifically to the surface. The spatial distribution of the protein on the aminophase surfaces may also play a role in encouraging non-specific binding of antigen to the surface. AFM analysis has shown that aminophase surfaces possess punctate regions, or islands, of protein. This leaves much of the glass exposed prior to blocking the surfaces with BSA. The probability of BSA adsorbing onto the exposed glass is limited by steric hindrance of the punctate protein regions and the relative hydrophilicity of the aminophase surface. This leads to the hypothesis that more of the glass surface is exposed after aminophase treatment, leading to greater non-specific binding of antigen to the surface.

For adsorbed and aminophase surfaces, the DNP-BSA MS showed a significantly higher amount of non-specific binding compared to BSA MS. This result could be an effect of charge interactions taking place at the surface due to the fact that DNP possesses several oxygen atoms, which resonate. Resonance induces partial negative charges around the oxygen atoms that may interact with partial positive charges present at the surface (amine groups on aminophase surfaces and exposed positively-charged residues present on adsorbed protein surfaces). Fig. 4 shows a 2,4-dinitrophenol molecule to illustrate the abundance of oxygen atoms present along with their partial charges (δ^-).

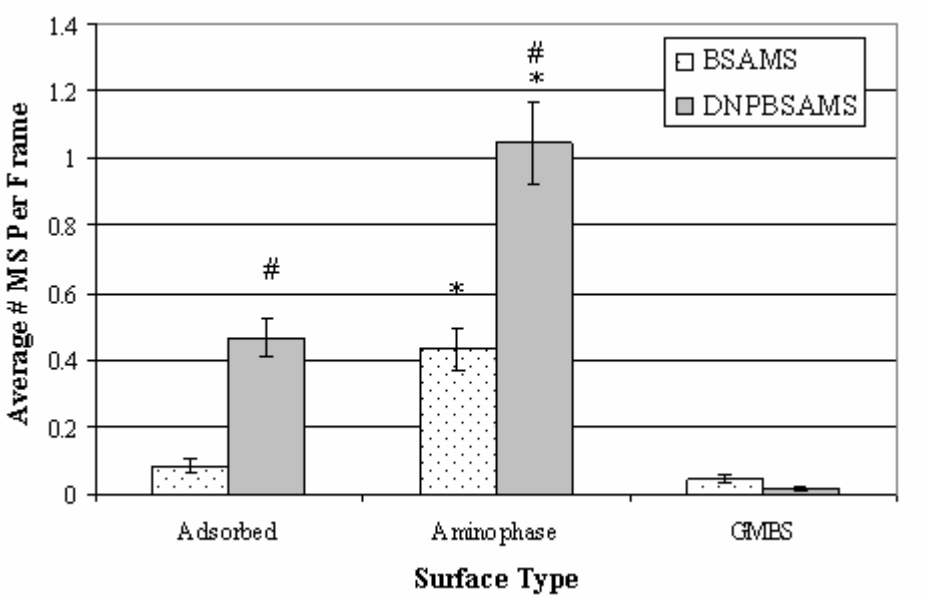

Figure 3: Non-specific binding of antigen to protein A + BSA surfaces, mean +/- SEM, n=3. *Significant increase in non-specific binding compared to GMBS and adsorbed surfaces, $p<0.05$. #Significant increase in non-specific binding

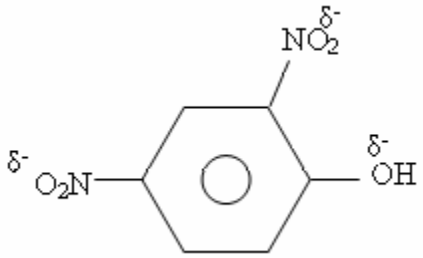

Figure 4: 2,4-Dinitrophenol schematic (adapted from Brown & Foote, 1998).

In the case of GMBS, however, there was no significant increase in the number of DNP-BSA MS bound compared to BSA MS on the control surfaces. More importantly, the non-specific antigen capture on the GMBS surfaces was lowest for both MS types compared to aminophase and adsorbed surfaces. GMBS is a large chemical molecule consisting of an aromatic ring with resonating oxygen atoms (see Fig. 1). As the GMBS molecule resonates, it could expose partial negative charges at the surface where it is bound. These partial negative charges could repel the DNP-BSA MS, which are partially negatively charged as well, due to like-charge repulsion. Steric hindrance (size effects) may also play a role in repelling the DNP-BSA MS away from the surface due to the high molecular weight associated with GMBS (MW 280.23).

The surface characteristics of the immuno-surfaces may have influenced the non-specific binding on the control surfaces in addition to the abovementioned factors. The variability in surface roughness on GMBS-protein A surfaces (Table 3) and the high surface area (Table 4) may have increased the effect of steric hindrance, thereby decreasing the non-specific binding of antigen to the surface. Additionally, the aminophase immobilization method yielded 3.02 $\mu g/cm^2$ of protein for the protein A + BSA surfaces but exhibited the greatest non-specific binding compared to the adsorbed method, which attached a similar amount of protein (2.16 $\mu g/cm^2$) and exhibited the median non-specific antigen capture. From previous observations, it

has been noted that the spacing of proteins on the aminophase surfaces is such that much of the glass is exposed to the antigen. This would most likely lead to non-specific binding at the surface. AFM images of protein A adsorbed to glass surfaces (Fig. 2) have shown that the protein spreads evenly over the surface while aminophase surfaces possess punctate regions of protein. This may explain why adsorbed surfaces, with similar protein density, exhibit lower non-specific binding than aminophase surfaces. It is also probable that several factors contribute simultaneously to the non-specific binding of the antigen to the surfaces including protein density, hydrophobic interactions, charge interaction, and steric hindrance. Although the exact mechanisms behind the non-specific binding trends observed in Fig. 3 remain unclear, the overall effect was experimentally demonstrated: non-specific binding was highest for the aminophase control surfaces and lowest for GMBS control surfaces.

1.2.2 Specific Interactions - Experiments testing the functionality of active immuno-surfaces showed that among the immuno-surfaces without protein A, the aminophase preparations performed best with the highest specific antigen capture (Fig. 5). This increase in antigen capture for the aminophase surfaces without protein A can be explained through the aminophase surface chemistry. It has been shown in the literature that there is a concentration of carbohydrate groups associated with the antibody's Fc region (Shriver-Lake *et al.*, 1997). The aminophase chemistry forms a bond between the amine group immobilized on the surface and the carbohydrate groups, specifically the carbonyl carbons, on the antibodies through an EDC reaction. By discriminately immobilizing the Fc region of the antibodies to the surface, the aminophase chemistry is able to orient the antibodies on the surface, allowing for greater accessibility of antigen-binding sites on the antibodies and a significant increase in SAC as shown in Fig. 5. This has also been shown experimentally by Chen *et al.* (2003). Among the immuno-surfaces with protein A, the adsorbed immuno-surfaces exhibited increased antigen capture when compared to the aminophase immuno-surfaces.

In the adsorbed and GMBS cases, there was a significant increase in SAC when the IgG + BSA and protein A + BSA + IgG preparations were compared using ANOVA and Duncan's multiple range tests. This increase in capture was most likely due to the improved orientation of the antibodies on the protein A immuno-surfaces. Surprisingly, orienting the antibodies with protein A did not always enhance antigen capture. When protein A was present on the aminophase surfaces, there was no increase in SAC. In fact, the aminophase-IgG_{2a}αDNP + BSA surfaces captured more antigen than the aminophase-protein A + BSA + IgG_{2a}αDNP surfaces. The surface preparations examined here, however, vary in their ability to immobilize antibody. To adequately compare the immobilization methods for their immuno-surface functionality, SAC was normalized to the amount of immobilized antibody achieved with each method.

The log of the resulting normalized specific antigen capture is shown in Fig. 6. This figure illustrates the antigen capture per amount of antibody immobilized and essentially eliminates any fluctuation in antibody density as a result of the surface attachment method utilized. Fig. 6 demonstrates the importance of protein A in increasing the functionality of the immuno-surface, as the capture on PA + BSA + IgG surfaces greatly exceeded the capture on IgG + BSA surfaces alone. Here it is shown that the most functional surfaces per antibody are those in which protein A is employed.

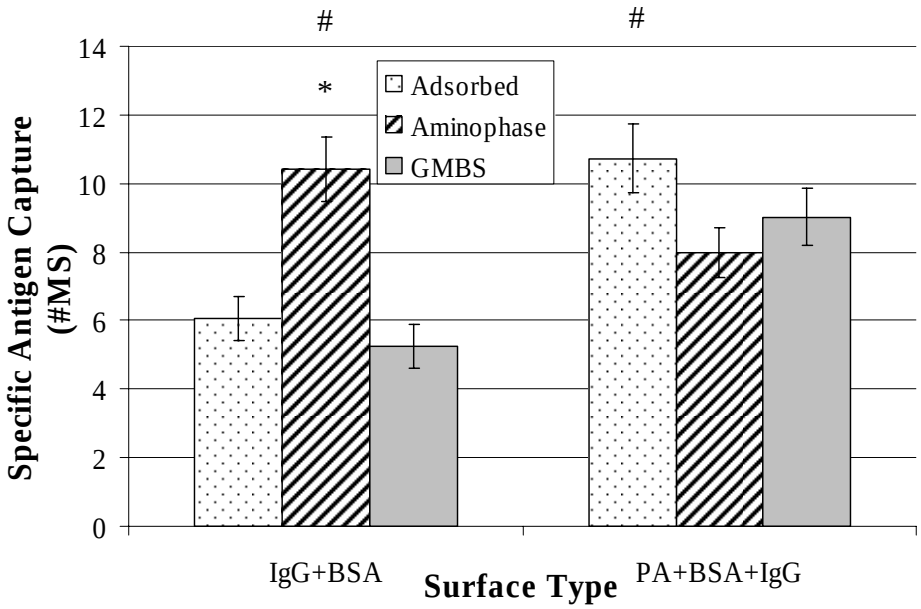

The aminophase-PA + BSA + IgG_{2a}αDNP immuno-surfaces exhibited the highest log of normalized antigen capture within the protein A + BSA + IgG group which contrasts with the result shown in Fig. 5. In the case of the aminophase-IgG_{2a}αDNP + BSA immuno-surfaces (Fig. 5), the aminophase chemistry most likely oriented the antibodies on the surface and increased antigen capture. As for the aminophase-PA + BSA + IgG_{2a}αDNP immuno-surfaces (Fig. 6), it is hypothesized that improved orientation due to the presence of protein A most likely improved antigen capture on aminophase-protein A + BSA + IgG_{2a}αDNP immuno-surfaces.

Although the GMBS immuno-surfaces have the highest amount of immobilized antibody they are not the most functional surfaces when antigen capture is evaluated in conjunction with antibody density. This result leads to the hypothesis that the majority of IgG_{2a}αDNP immobilized via GMBS without protein A is not functional and, therefore, blocking the surface rather than actively capturing antigen.

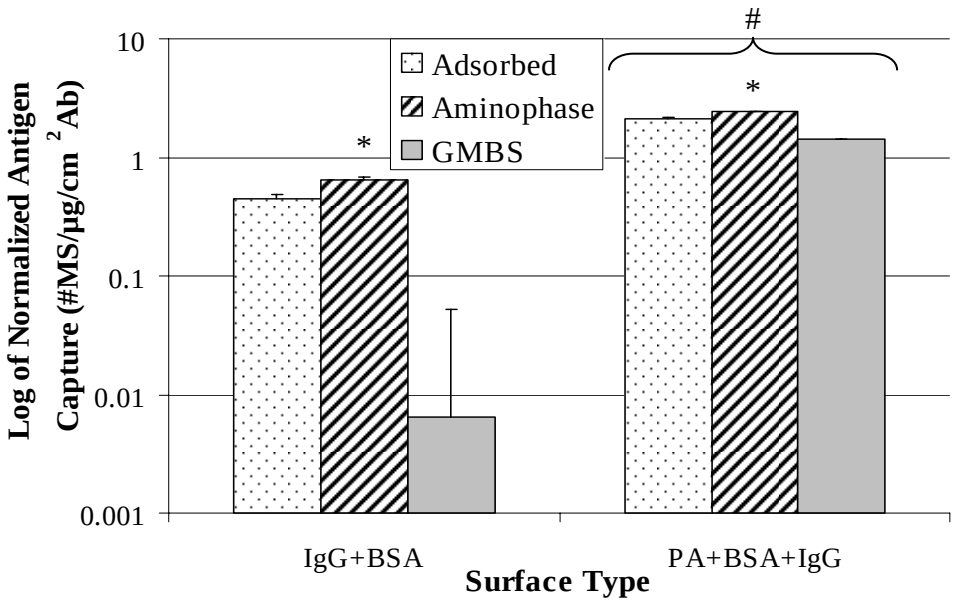

Figure 6: Log of normalized SAC for active immuno-surfaces, +SEM, n=3. *Aminophase IgG + BSA immuno-surfaces showed a significant increase in log of normalized SAC compared to GMBS IgG + BSA immuno-surfaces, aminophase protein A + BSA + IgG immuno-surfaces showed the highest log of normalized SAC compared to adsorbed and GMBS protein A + BSA + IgG immuno-surfaces, $p<0.05$. #Significant increase in log of normalized SAC for all protein A + BSA + IgG immuno-surfaces compared to all IgG + BSA immuno-surfaces, $p<0.05$.

1.3 Conclusions to Section 1

This study compares three different antibody immobilization methods for their antigen capture performance. When directly immobilizing the antibodies, the aminophase immuno-surfaces exhibited the most specific antigen capture; however, when immobilizing protein A as a scaffold to orient antibodies, the adsorbed immobilization method exhibited an increase in specific antigen capture when compared to aminophase surfaces only. The presence of protein A improved the capture capabilities of the adsorbed and GMBS surfaces but protein A did not increase antigen capture on the aminophase surfaces. This effect may be attributed to the aminophase surface chemistry targeting the Fc regions on the antibodies to effectively orient them.

The experiments show that the amount of antibody immobilized on the protein A immuno-surfaces is less than the amount of antibody immobilized directly onto the surface for each immobilization technique. Normalization to the antibody surface density further confirms the importance of protein A in increasing the functionality of the immuno-surface. This result suggests that protein A is able to orient the antibodies allowing for greater antigen capture per antibody present on the surface. By increasing the efficacy of the antibodies immobilized on the surface with protein A, antibody immobilization becomes more cost effective by allowing for

antibody retrieval after immobilization and reducing the amount of antibodies that are blocking the surface rather than capturing antigen.

AFM analysis showed that the aminophase chemistry immobilized protein A such that punctate regions were present on the surface. This result supports the conclusion that the aminophase immobilization treatment increases non-specific antigen capture by increasing the probability of antigen interacting with uncoated glass regions on such surfaces. Adsorbed protein A surfaces were uniform and smooth compared to glass alone and aminophase and GMBS surfaces. Additionally, GMBS showed great variation in surface roughness between locations while aminophase and adsorbed surfaces were more consistent between random locations examined. The variation of GMBS surface roughness and the large apparent surface area may reduce non-specific antigen capture as steric hindrance may be elevated for such surfaces.

Antigen capture experiments performed on aminophase control surfaces showed the highest non-specific binding for DNP-BSA and BSA MS compared to GMBS and adsorbed surfaces. The non-specific binding observed on aminophase surfaces may be attributed to the hydrophilicity of the surface and the punctate nature of the surface, while the adsorbed showed less non-specific antigen capture due to the near-complete coverage of the surface with protein A. GMBS control surfaces showed the lowest non-specific binding. This may be due to steric hindrance between the GMBS molecules and the MS, or other surface-protein interactions, acting alone or in combination.

These results demonstrate and explore many of the issues associated with determining the best protein scaffold design for improving biosensor specificity, selectivity, and sensitivity. Although glass was chosen as the experimental substrate, various other materials including polymers and ceramics are being explored in immuno-surface applications. Decisions regarding choice of immobilization method, antibody surface density, and immuno-surface functionality depend on the material chosen for the surface. For example, aminophase and crosslinker techniques utilize solvents that are incompatible with polymers but work well with ceramics such as glass. One other drawback is that these harsh solvents interact with the antibodies in the procedure, thereby eliminating the possibility of antibody retrieval and increasing the amount of wasted antibodies. If a polymer is to be used, adsorption of protein A or the design of a custom crosslinker may be the best technique to immobilize antibodies and retain their function.

This work has shown that the immuno-surface with the highest functional antibody density exhibits the greatest specific antigen capture and limits non-specific binding of antigen to the surface. For example, the GMBS method immobilized the greatest amount of antibody and possessed the lowest non-specific binding, while the aminophase surfaces, which orient antibodies, captured the greatest amount of antigen per antibody. These observations illustrate the importance of antibody density and retention of antibody function as they are immobilized. Ideally, future immuno-surface designs should include a surface chemistry motif in which high antibody density and maximum antibody function are achieved to increase biosensor sensitivity. Here it was shown that protein A can increase antibody function on GMBS surfaces, which possess high antibody density, by improving antibody orientation; however, detection methods such as surface plasmon resonance are limited in sensitivity to detect antigen if the antibodies are located relatively far from the surface; this limits the use of protein A. As an alternative, a crosslinker possessing a chemical ring structure similar to that of GMBS could be designed in which the terminal end possessed an amine group similar to the aminophase scheme. By combining the high antibody density characteristic of GMBS with the aminophase method's

ability to orient antibodies, this custom-designed crosslinker could possibly achieve high antibody density and function simultaneously, thereby increasing biosensor sensitivity while limiting the distance between the antibodies and the sensor surface. Additionally, covalent immobilization adds stability to the immuno-surface design by decreasing the probability of antibody desorption.

2.0 Modeling Multivalent Antigen Binding Dynamics to Immobilized Antibodies

This work has generated a model that reflects multivalent antigen binding dynamics to immobilized antibodies. The model incorporates the effective far-field antibody surface density, the local antibody surface density once the antigen is bound, and the flexibility and functional range of motion of the immobilized antibodies. Each of these contributions is described within this section through a series of stepwise developments towards an increasingly more complex model that reflects the multivalent-antigen binding to a biosensor immuno-surface. Although important, this work neglects the antigen transport dynamics as this is addressed in many other publications [Edwards et al. 1999, Mason et al. 1999, Myszka et al. 1998, Paek et al. 1991,Vijavendran et al. 1999] to name a few. For simplicity, an idealized well-mixed model of antigen transport is used which assumes the proximal antigen concentration near the immuno-surface remains constant during the association phase and zero during the dissociation phase; this enables the theoretical isolated evaluation of other immuno-surface factors that influence the antigen capture.

2.1 Model Development

2.1.1 Far-field Antibody Surface Density - Upon antigen binding, the effective antibody surface density decreases since fewer antibodies are now available. Reflection of this effect in the model requires the incorporation of an effective antibody surface density which decreases as antigen are bound. Several studies have approximated the free antibody surface density, R_f, as a decreasing function of bound antigen, x_i, as $R_I = R_f + \sum_{i=1}^{f} i\, x_i$ where R_I is the initial antibody surface density [Hlavacek et al. 1999, Perelson et al. 1980, Sulzer et al. 1996]. This approximation is sufficient when there is little or no crosslinking as is the case for haptens or small ligands, when the antibodies are mobile, or when the immobilized antibodies are sparse. However, when considering the capture of larger antigen such as viruses or bacteria that can range from nanometer to micron sizes, there are considerably more antibodies blocked than there are antibodies that are bound. Thus the reduction in available antibodies, not simply bound antibodies, is used as an estimate of the effective surface density, also referred to as the far-field antibody surface density.

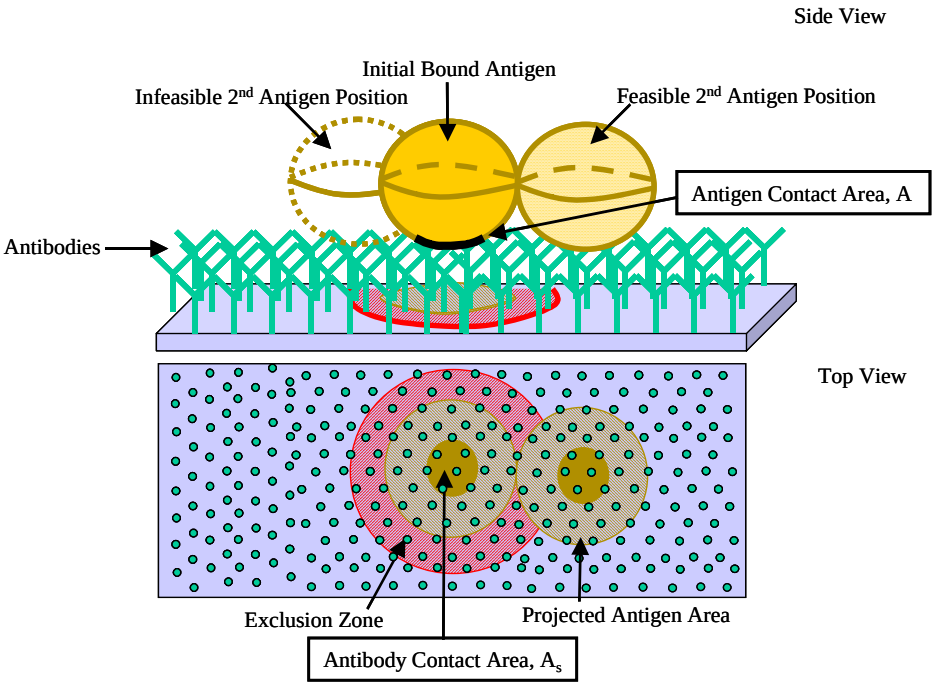

Figure 7: Blocking and exclusion of immobilized antibodies from bound antigen

When an antigen is bound to the immuno-surface, a portion of its area is within close proximity of the active surface and available for a surface-surface reaction. The surface area reachable by the immobilized antibodies is referred to as the antigen contact area, A, see Fig. 7 for an illustration. The antibodies that are available to bind to the bound antigen are those within the antibody contact area, A_s, that are not currently bound or blocked by another bound antibody. The far-field antibody surface density, R_f, reflects the steric hindrances; the bound antigen blocks all antibodies that are located within the antigen projection area from binding to other antigen. Although some of these antibodies are unbound, they are not accessible to any other antigen. This decreases the effective surface density of free antibodies. Thus the density of available antibodies is a function of the number of bound antigen and its dimensions. An approximation of this effect is given by:

$$R_f = R_I(1-N_a x_b P_{AG}) \quad (1)$$

where R_I is the initial antibody surface density, N_a is Avogadro's number to convert moles to the number of bound antigen, $x_b = \sum_{i=1}^{f} x_i$ is the bound antigen surface density, and P_{AG} is the projected area of the antigen on the immuno-surface.

A less conservative alternative approximation can be made by applying the same approach used for Hlavacek, Posner, and Perelson's model of epitope availability [Hlavacek et al 1999]. The immobilized antibodies not available for binding to additional antigen include those contained within the projected antigen area as well as the bordering antibodies. A bound antigen creates an exclusion zone that extends beyond its projected area, see Fig. 7. For a spherical antigen the effective far-field antibody surface density is estimated as $R_I P(\text{available})$ where R_I is the initial surface density and P(available) is the probability that they are available. This

probability is given by the product of the probability a receptor is not bound, $P(\overline{B})$, the conditional probability it is not covered given it is not bound, $P(\overline{C}/\overline{B})$, and the conditional probability it is not excluded given it is neither covered nor bound, $P(\overline{E}/\overline{C}\,\overline{B})$. For a spherical antigen on a randomly distributed antibody surface, the effective antibody surface density can be estimated as:

$$R_f = R_I P(\text{available}) = R_I\left(1-\frac{M}{R_I S N_a}\right)\left(1-\frac{M\pi r^2}{S}\right)\left(1-\frac{3\pi r^2}{S-M\pi r^2}\right)^M \qquad (2)$$

where R_I is the initial antibody surface density, N_a is Avogadro's number, $M = N_a \times S \times \sum_{i=1}^{f} x_i$ is the total number of antigen bound to the immuno-surface, r is the effective radius of the antigen, S is the total immuno-surface area.

This section has discussed the incorporation of the effective antibody surface density, the far-field antibody surface density. This imp15acts the model dynamics as the surface density drives the rate of initial an antigen association. This is purposefully differentiated from the local antibody surface density that controls the rate of multiple bond formations between the antigen and immobilized antibodies. The next section explores how each individual epitope binding decreases the effective local antibody density within the context of the model of multivalent antigen binding to a biosensor immuno-surface.

2.1.2 Local Antibody Surface Density - Modifications to the incorporation of antibody surface density were made to the Hlavacek, Posner, and Perelson's model to include the far-field and local effects of the immobilized antibody surface density. The revised model is stated below:

$$\begin{aligned}
\frac{dx_1}{dt} &= k_a x_0 R_f - k_{-1} x_1 - \upsilon(1) k_x x_1 R_L(1) + 2k_{-x} x_2 \\
\frac{dx_2}{dt} &= \upsilon(1) k_x x_1 R_L(1) - 2k_{-x} x_2 - \upsilon(2) k_x x_2 R_L(2) + 3k_{-x} x_3 \\
&\vdots \\
\frac{dx_f}{dt} &= \upsilon(f-1) k_x x_{f-1} R_L(f-1) - f k_{-x} x_f
\end{aligned} \qquad (3)$$

where x_0 equals a constant. The kinetics governing the binding of the multivalent antigen occurs in two stages. The first stage involves the rate of the initial antigen association that is proportional to the product of the antigen-antibody association rate constant, $k_a \approx Nk_1$, the far-field antibody surface density, R_f, and the proximal antigen concentration, x_0. Once bound the second stage involves the subsequent epitope crosslinking that is a function of the rate constant, k_x, the effective antigen valency, $\upsilon(i)$, and the effective local antibody surface density (near the bound antigen), R_L.

The original Hlavacek, Posner, and Perelson's model was derived for antigen binding to mobile, renewable cell-surface receptors. Thus, the original model assumes that the receptors are not limited locally and are replenished in depleted areas. However, for immuno-assays and most immuno-based biosensors, the antibodies are immobilized and not replenished, thus our local antibody surface density has a different interpretation. The local surface density is given as the surface density of antibodies available and capable of binding to the bound antigen. Thus, the local antibody surface density will decrease with each bound receptor as:

$$R_L(i) = R_I - \frac{i}{A_s N_a} \tag{4}$$

where R_I is the initial antibody surface density, A_s is the antibody contact area, i is the bound epitope index, and N_a is Avogadro's number to convert the number of bound antibodies to moles. The effects of this modification are minor when only a few antibodies exist within the antibody contact area or a few epitopes are presented in the antigen contact area. Nevertheless, this modification makes the antigen capture and dissociation rate more realistic when multiple epitopes are bound within the antigen contact area.

2.1.3 Immobilized Antibody Flexibility and Range of Motion - An individual immobilized antibody cannot reach all of the antigen epitopes within the antigen contact area: there are a limited number of reachable epitopes per immobilized antibody. Another model enhancement takes this limitation into account by estimating the reachable region for each immobilized antibody.

Antibodies come in a variety of types; the primary type used for immuno-based biosensors is IgG. The structure of IgG is shown in Fig. 8. There are two binding sites per antibody called paratopes: each site will bind an epitope of the antigen. IgG antibodies are inherently pliable. IgG antibodies comprise two heavy chains and two light chain polypeptides connected together at a flexible hinge region (comprising two dissulfide bonds and enriched in proline, serine, and threonine) [Harlow et al 1999]. This hinge provides a large amount of segmental and axial (torsional) flexibility (nearly 0 - 180^o [Schumaker et al 1991, Wade et al. 1989]) for the antibody binding sites to potentially bind to two different epitopes on a single antigen. Thus there is a feasibility region defined by this range of motion and any antigen epitopes that contained within this space may become bound by a free antibody in that area. Depending upon the antibody immobilization method, the antibody may exhibit even a larger range of motion and have a flexible joint its the base. In this instance the antibody binding region is substantially larger than that for Fab arm mobility as illustrated by the total antibody flexibility in Fig. 8.

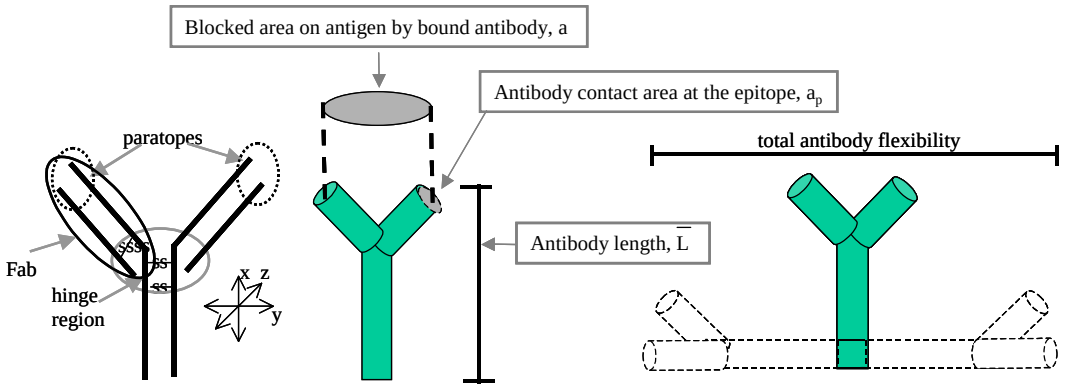

Figure 8: Structure of an IgG antibody and a schematic of the antibody flexibility

This concept of a feasibility region can be integrated within the framework of the model stated in equation 3 by modification to $\upsilon(i)$ replacing the total number of epitopes available within the antigen contact area, n, by the number of epitopes available locally to any individual antibody, q.

$$\upsilon(i) = qP_i(\text{available}) = q\left(1-\frac{i}{n}\right)\left(1-\frac{ia}{A}\right)\left(1-\frac{3a}{A-ia}\right)^i \tag{5a}$$

The number of epitopes reachable by an individual antibody can be estimated as:

$$q = \left(\left(\overline{Q} - a_p\right)\varphi + a_p\right)\rho \tag{5b}$$

where a_p is the antibody contact area at the epitope, $\overline{Q}$ is the mean reachable antigen contact area for an individual antibody, ρ is the epitope density on the antigen, and φ is the antibody flexibility. Incorporation of the antibody immobilization and flexibility within this model requires an estimate of $\overline{Q}$, the feasible mean reachable area on the antigen by the antibodies within the antibody contact area, A_s. These parameters depend upon the dimensions and flexibility of the antibody and the spatial characteristics of the antigen.

In addition, the flexibility of the antibody is a function of the antibody immobilization method and limited by the antibody surface density. As the antibodies are packed tighter together they interfere with one another and inhibit full range of motion of an antibody. In this model, each antibody is considered as monovalent with its flexibility limited as the antibodies are packed more densely on the surface. The distance separating the immobilized antibodies can be estimated as $d = \sqrt{\frac{1}{R_I N_a}}$ where R_I is the initial antibody surface density and N_a is Avogadro's number. Our model assumes that the decrease in flexibility of the antibody is linearly proportional to the decrease in antibody spacing as:

$$\varphi = \gamma \times \begin{cases} 0 & d < \sqrt{a} \\ \dfrac{d-\sqrt{a}}{\overline{L}} & \sqrt{a} \le d \le \overline{L} + \sqrt{a} \\ 1 & d > \overline{L} + \sqrt{a} \end{cases} \tag{6}$$

where γ is the maximum flexibility afforded by the antibody immobilization method, $\overline{L}$ is the antibody length, $\sqrt{a}$ is the effective width of the Fab arm, and d is the average distance separating the immobilized antibodies.

2.2 Results and Discussion

This section demonstrates the model enhancements through a series of simulation results and discussion. Equation 3 states the model being investigated with enhancements to the definition of $\upsilon(i)$ with equations 5 and 6. All simulations were run in MATLAB™ version 6.0.0.88 using a stiff differential equation solver based on numerical differentiation formulas. The assumptions used to construct the fundamental model from Hlavacek, Posner and Perelson's model [Hlavacek et al 1999] must also hold for this enhanced model. This implies that the antibody contact area at the epitope must be much smaller than the antigen contact area, a << A. In addition, to accommodate the situations which arise when there are more antibodies available than antigen epitopes or the antibody contact area (A) is fully occupied with bound or excluded antibodies, the probability of an available antibody, $0 \le P_i(\text{available}) \le 1$ for all i, from equation 4 and 5a is constrained to be greater than or equal to zero and less than or equal to one.

The surface density of bound antigen quantifies the results. A bound antigen has at least one epitope bound within the antigen contact area A, and is computed as $x_b = \sum_{i=1}^{f} x_i$ with surface density units, moles per dm^2. As most biosensor and diagnostic tests rely upon a dissociation period to remove non-specifically bound antigen, the antigen capture, as defined herein, considers both the amount of antigen bound to the surface during the association phase and the ease with which the bound antigen is removed from the immuno-surface during the dissociation phase. Thus both the association and dissociation phases are shown for most simulation results. The antigen dissociation is characterized by a lumped antigen dissociation rate which does not equal the dissociation rate constant but rather is a function of the extent of crosslinking.

For simplicity, these simulations were completed assuming a spherical antigen with uniformly spaced epitopes: many types of spores are spherical; other shaped bacteria or viruses can be approximated by an effective diameter so that the projected and excluded areas are similar to a spherical antigen.

In this section, the model rate parameters were kept constant even though the model structure was modified in a step-wise manner to help evaluate the effects of each modification. The model parameter descriptions and values used for these simulations are stated in Appendix I. It should be noted that the nominal affinity of the antibody utilized for these simulations is quite low (on the order of $k_a/k_{-1} = 10^6$ M^{-1}); this value was specifically selected to demonstrate the impact of our modeling refinements and the potential biosensor enhancements explored in a later section. It is well known that identified model rate parameters are highly dependent upon the model structure thus when the model is modified, the rate parameters may change significantly with their interpretation.

2.2.1 Illustration of the Far-field Antibody Surface Density Effects - The results presented in this section illustrate the importance of incorporating the far-field antibody surface density and the antigen size effects in models of antigen capture. Initially, a comparison of the four methods to model the far-field antibody surface density are compared for a 0.5 micron diameter spherical antigen: (i) constant antibody surface density, (ii) decreased by the number of bound antibodies, (iii) reduced by the number of antibodies within the bound antigen projected area (equation 1), and (iv) reduced by the number of antibodies within the projected area plus an additional exclusion zone (equation 2). The simulations, shown in Fig. 9a, investigate the antigen capture dynamics of the association phase (first 100 seconds) and the dissociation phase ($t > 100s$). As expected, there are substantial differences resulting in the simulation results depending upon how one incorporates the far-field antibody density affect on the antigen capture. For the first case, when the far-field antibody surface density is assumed to remain at its initial level, R_I, the antigen association is not inhibited and will exponentially grow until reaching equilibrium. When the surface density of available immobilized antibodies is reduced by the number of bound antibodies, $R_f = R_I - \sum_{i=1}^{f} i x_i$, the antigen binding is moderated by the decrease in available antibodies. In the remaining two cases, the projected area and the exclusion area models, show an even more significant reduction in antigen binding as a result of previous antigen bound. The exclusion model and the projected area model results are quite similar, although as expected the exclusion zone is more limiting, see the inset image in Fig. 9a.

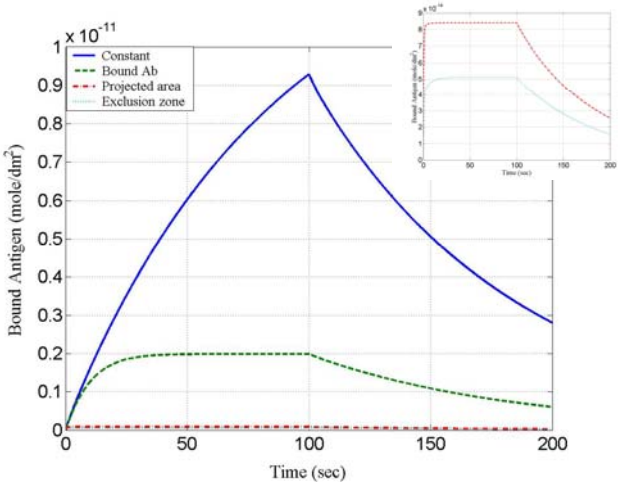

Figure 9a: Comparison of various far-field antibody surface density representations

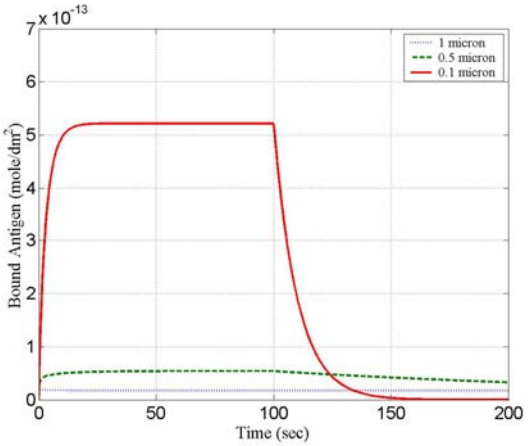

Figure 9b: Comparison of antigen size effects with the exclusion zone model

Both the projected area and the exclusion zone methods are direct functions of the antigen size while the other methods are indirectly associated with it through the computation of the f and n, the number of antibodies and epitopes within the contact area respectively. Without consideration to the area occupied by each bound antigen, both the constant antibody surface density and the reduction upon bound antibody models violate a conservation of area; for antigen larger than the antibody, the total surface area occupied by bound antigen may exceed the total surface area of the active immuno-surface. With the projected area and the exclusion zone model, for large antigen the equilibrium is dictated by available space on the surface while for smaller antigen the relative association and dissociation rate constants dictate the equilibrium level (Fig. 9b). When the antigen epitope density is constant, regardless of the antigen size, the dissociation rate of the larger antigen is slower than that for the smaller antigen due to the increased antigen contact surface area and more crosslinking.

As a result of these simulations, it can be concluded that antigen size plays an important role in antigen capture and cannot be neglected. The antigen projection area model provides an upper bound on the predicted level of antigen capture while the exclusion zone model provides a more realistic estimate. The remainder of this section will continue to refine the exclusion zone model.

2.2.2 Illustration of the Local Antibody Surface Density Effects - The results presented in this section illustrate the impact of incorporating the local antibody surface density in models of antigen capture, building upon the exclusion zone model explored in the previous section. Fig. 10 provides a graphical comparison of the antigen capture for the 0.5μm spherical antigen with and without accounting for the reduction in local antibody density. As expected, a reduction in available antibodies to bind within the antigen contact area slightly reduces the antigen association by approximately 5% at the end of the association phase; in addition, the lumped antigen dissociation rate increased reflecting the fact that fewer antibodies are bound. This modification has no effect when the number of epitopes available within the antigen contact area is unity or the effective antigen diameter is small and only one antibody can bind (results not shown). Again, although this inclusion of the local antibody density causes a slight change to the

equilibrium level during the association phase, it has refined the lumped dissociation rate for the model of multivalent antigen binding to a biosensor immuno-surface.

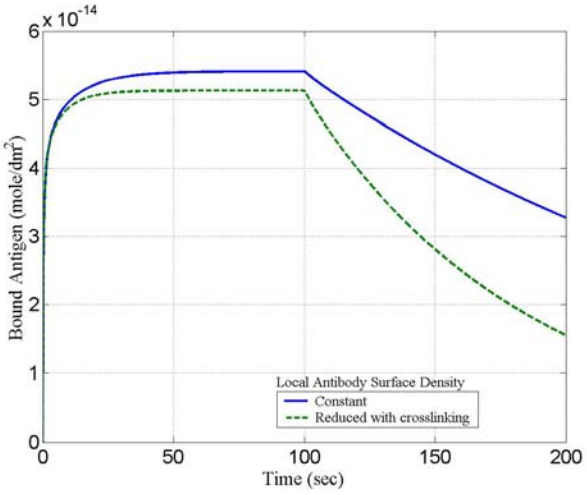

Figure 10: Effects of incorporating the local antibody surface density

2.2.3 Illustration of the Antibody Immobilization - Incorporation of the antibody immobilization within the model requires an estimate of $\overline{Q}$, the mean reachable area on the antigen by each antibody within the antibody contact area, A_s. This depends upon the dimensions and flexibility of the antibody as well as the spatial characteristics of the antigen. Initially, the antibody is assumed to exhibit total (100%, $\varphi = 1$) flexibility. The reachable area within the antigen contact area, A, within the antibody contact area, A_s, is different for different antibodies, see Fig. 11a.

The antibody contact surface area is computed as the area of a circle with radius r_0, see Fig. 11b. The radius of the antibody contact surface area as a function of antibody length, $\overline{L}$, and antigen radius, $\overline{R}$, is given by:

$$r_0 = \sqrt{\left(\overline{R}+\overline{L}\right)^2 - \overline{R}^2} = \sqrt{\overline{L}^2 + 2\overline{RL}}$$

so the antibody contact surface area is

$$A_s = \pi r_0^2 = \pi\overline{L}^2 + \overline{RL}.$$

The antigen contact area for a spherical antigen can be estimated as:

$$A = 2\pi\overline{R}^2(1-\cos\phi) = 2\pi\overline{R}^2\left(1-\frac{\overline{R}}{\overline{R}+\overline{L}}\right) = \frac{2\pi\overline{R}^2\overline{L}}{\overline{R}+\overline{L}}.$$

An antibody at position r has a reachable area Q(r) that is estimated as

$$Q(r) = 2\pi\overline{R}^2(1-\cos\theta) + a_p \quad \text{where} \quad \cos\theta = \frac{\left(\overline{R}^2+r^2\right)+\overline{R}^2-\overline{L}^2}{2\overline{R}\sqrt{\overline{R}^2+r^2}}$$

and a_p is the antibody contact area on the antigen at the epitope. Thus

$$Q(r) = 2\pi\overline{R}^2\,\frac{\overline{L}^2-\left(\sqrt{\overline{R}^2+r^2}-\overline{R}\right)^2}{2\overline{R}\sqrt{\overline{R}^2+r^2}} + a_p$$

.

This formulation ensures that the minimal reachable area by a given antibody within A_s is the antibody contact area at the epitope, a_p. Since each antibody's reachable area depends upon where it is located within the antibody contact area, Q is estimated by the mean reachable area in

equation 5b. The reachable area for each antibody within the antibody contact area is equivalent for all antibodies on concentric circles centered about the contact point, thus the mean reachable area can be estimated by

$$\overline{Q} = \frac{1}{\pi r_0^2}\int_0^{r_0} Q(r)\times 2\pi r\,dr \;= \frac{4\pi\overline{RL}^2}{3\left(\overline{L}+2\overline{R}\right)}+a_p$$

where r_0 is the distance of the furthest antibody from the contact point which can still reach the spherical antigen.

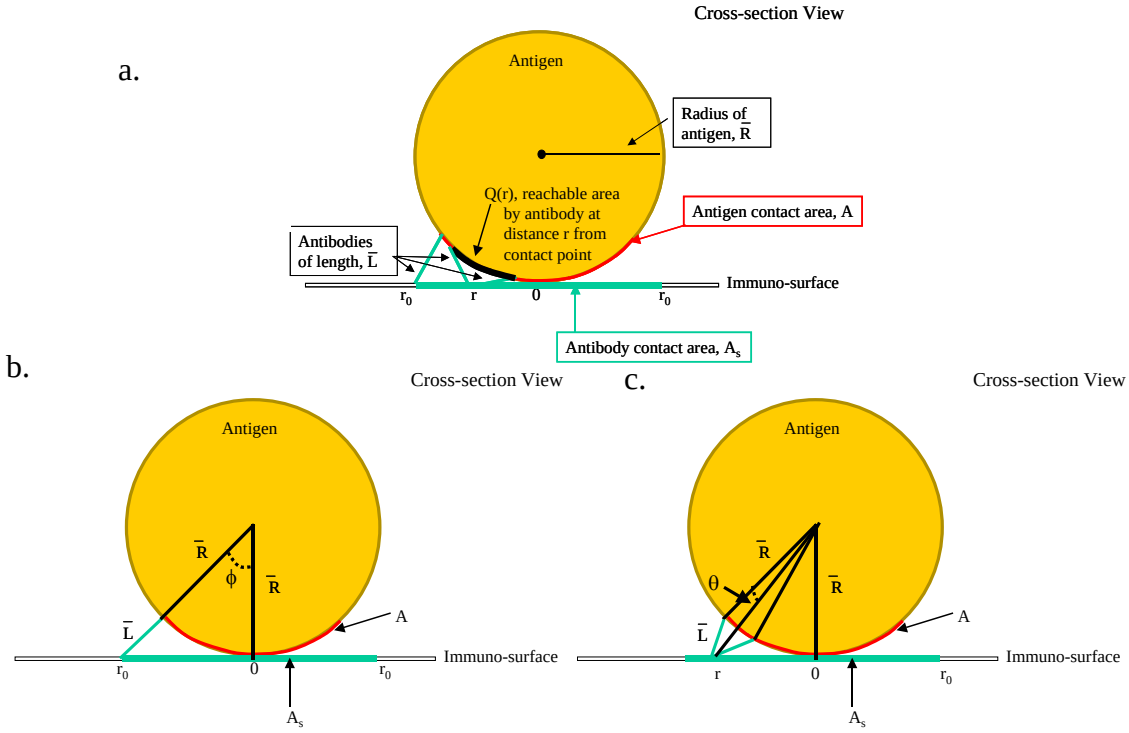

Figure 11: a. Reachable area by an antibody at distance r from the contact point, b. Antibody contact area estimation, c. Simplified cross-sectional image for reachable area estimation

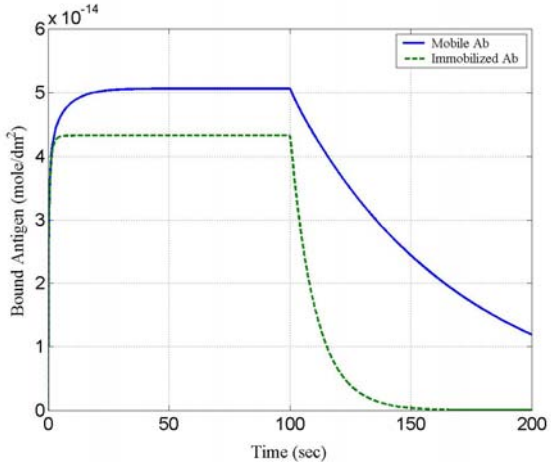

Figure 12: Effects of immobilizing the ntibodies

Removing the inherent assumption that all antibodies can interact with any epitope within the antigen contact area limits the number of crosslinking events thereby increasing the antigen dissociation rate. The results of incorporating this limitation within our model that includes the exclusion zone and the local antibody density can be seen in the simulation results in Fig. 12. For this particular example, $\upsilon(i)$, the number of epitopes that are available in the i^{th} step in the crosslinking process is substantially reduced by the limitation on individual antibody reach.

2.2.4 Illustration of the Antigen Valency Effects - With the inclusion of the feasible antibody reach area, the effects of antigen valency can be investigated. The epitope surface density on the antigen, ρ, plays a large role in the probability of crosslinking events. Fig. 13 illustrates, the model's response to different epitope surface densities for a 0.5 micron sphere. Not surprisingly, for higher epitope surface densities, the immuno-surface captures more antigen during the association phase and releases it more slowly during the dissociation phase as more epitopes are bound. For smaller antigen epitope densities, the binding is dominated by the first binding event as is the case when ρ = 1e13 and 1e15 epitopes/dm^2 since the immobilized antibodies effectively see only a few epitopes. For the lower epitope surface density cases as only one epitope is bound per antigen, the equilibrium level can be predicted by solving the nonlinear equation 3 for x_1 when $dx_1/dt = 0$:

$$x_1 = \frac{k_a x_0}{k_{-1}} \left(R_I \left(1 - \frac{x_1}{R_I \times S \times N_a} \right) \left(1 - \frac{x_1 \pi \bar{R}^2}{S} \right) \left(1 - 3 \frac{\pi \bar{R}^2}{S - x_1 \pi \bar{R}^2} \right)^{x_1} \right)$$

where S is the total immuno-surface area. This comparison of the antigen capture dynamics for high and low epitope surface densities serves as an illustration of the importance on crosslinking to reduce the lumped antigen dissociation from the immuno-surface even though the antibody-epitope association and dissociation rate constants are equivalent and constant.

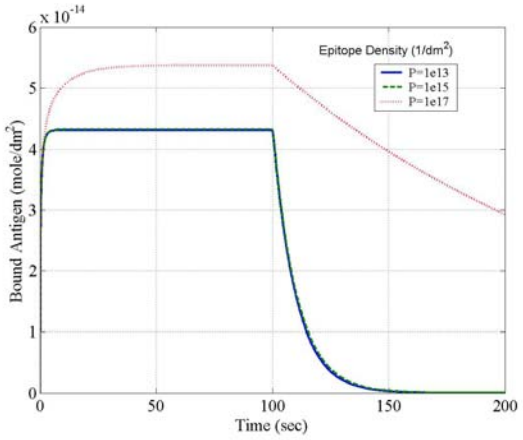

Figure 13: Illustrating the effect of epitope density on antigen capture

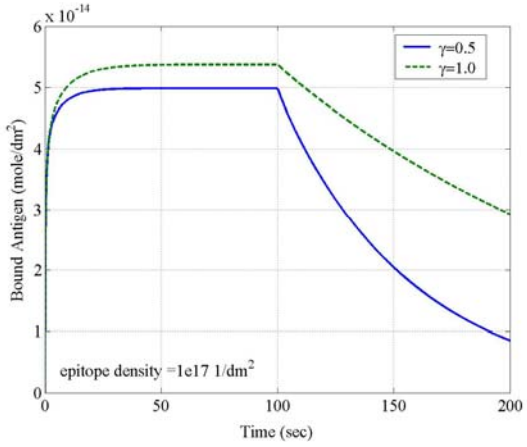

Figure 14: Incorporation of limited antibody flexibility on antigen capture

2.2.5 Illustration of the Antibody Flexibility Effects - The flexibility of the antibody will depend upon the immobilization technique and the antibody density. These effects were incorporated in the model through equation 6. The immobilization technique constrains γ, the maximum flexibility (between $0 \leq \gamma \leq 1$). While, the decrease in flexibility as a result of the antibody surface density is assumed to be linearly proportional to the decrease in antibody spacing. The restriction of the antibody flexibility essentially limits the reachable area by the immobilized antibodies. These effects are demonstrated in Fig. 14. By limiting the antibody flexibility, there is a reduction in antigen capture as the antibodies cannot reach multiple epitopes on the antigen surface.

2.3 Biosensor Immuno-Surface Design

Immuno-based biosensors and diagnostic tests rely upon immobilized antibodies to capture and retain the specific target antigen and many of these utilize a wash or dissociation period to remove non-specifically bound antigen. The previous sections developed a model of multivalent antigen capture by a biosensor immuno-surface. In this section, the objective is to utilize this model to design immuno-surfaces that enhance antigen capture. To accomplish this, antigen capture must be defined more rigorously: it is a function of the amount of antigen bound to the surface during the association phase and the ease with which the bound antigen is removed from the immuno-surface during the dissociation phase. To a first order approximation, during the dissociation phase, the antigen being released from the immuno-surface can be estimated as an exponential decay $x_b(t_a)e^{-k_{DAg}t}$. This term provides a rough estimate of the amount of antigen retained on the surface at any point, t, in time during the dissociation phase for some lumped antigen dissociation rate k_{DAg} where t_a is the when time the association period ends. To compare different surfaces, antigen capture is defined as $x_c = x_b(t_a)e^{-k_{DAg}100}$. Clearly for larger wash or dissociation periods prior to the measurement the lumped antigen dissociation rate becomes more important. This measure considers both the amount captured during association as well as the lumped antigen dissociation rate.

For this study, the target antigen is assumed to be defined, thus the controllable properties are those of the immuno-surface such as the antibody affinity, the antibody surface density, antibody attachment, and the immuno-surface properties. Analyzing the developed model will help identify which controllable properties will enhance the immuno-surface antigen capture capabilities thereby maximizing the antigen capture at a particular point in time.

2.3.1 The Role of Antibody Affinity

Maximizing the affinity of the antibody enhances the antigen capture by the immuno-surface. Achieving the same high affinity antibodies can be accomplished by ratios of different association and dissociation rate constants. The developed model suggests that minimizing the dissociation rate constant plays a larger role than maximizing the association rate constant, this is shown in Fig. 15.

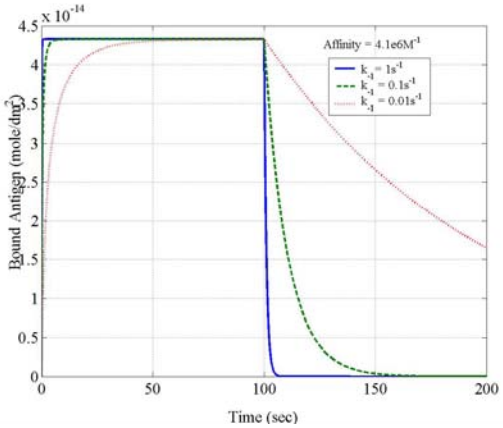

Figure 15: Comparison of antigen capture by equivalent antibody affinities differing in the association and dissociation rate constants

Once an association event takes place the multiple epitope bonds are formed rapidly due to the close proximity thus it is more important to prevent the antigen escape from the immuno-surface with a smaller dissociation rate constant. Interestingly, most antibodies produced by B-cells have fairly similar association rates and differ in their dissociation rates [Berzofsky et al, 1999] to achieve a large range of antibody affinities.

2.3.2 The Role of Antibody Surface Density - Ignoring the antibody flexibility, larger antibody surface densities promote antigen capture since more antibodies bind within the antigen contact area and slow the antigen dissociation. This result inappropriately suggests that maximizing the antibody surface density will enhance antigen capture. By incorporating the antibody flexibility, there is a reduction in antigen capture with increased antibody density as the antibodies loose their flexibility and cannot reach multiple epitopes on the antigen surface. This effect is in agreement with qualitative observations that suggests there is a limit to the effectiveness of high antibody surface densities. Interestingly, this result also suggests an optimal antibody density exists which is independent of the antigen-epitope spacing or density, see Fig. 16. (The non-smooth descent in this figure is a function of the integer values for the number of antibodies available, f, and the number of epitopes available, q.) Rather the optimal antibody surface density ($2.35e^{-11}$ mol/dm^2 = $14.2e^{12}$ antibodies/dm^2) maximizes the surface density without reducing the antibody flexibility; the antibodies are spaced by roughly double the antibody length ($2.4*1.1e^{-7}$dm). On the surface of a B-cell, there are about 100,000 antibodies [Alberts et al 2002], and the cell has about $32e^{-9}$ dm^2 surface area, thus on average (prior to immune-synapse formation) the antibodies are uniformly distributed at $3.12e^{12}$ antibodies/dm^2 with a spacing of about $5.6e^{-7}$dm which is only about double the distance apart than for the optimal surface density of immobilized antibodies. The B-cell antibody surface density is about 1/5 the optimal immobilized antibody surface density. It intuitively makes sense that fewer mobile antibodies are required to capture the antigen as they can move to adjust after the initial binding event.

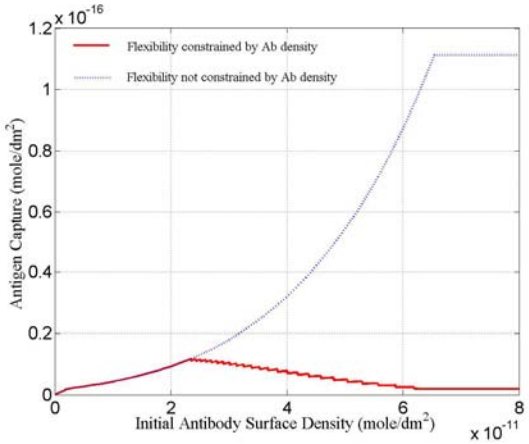

Figure 16: Effects of antibody surfacedensity on antigen capture where A_s is the antibody contact area.

Additional factors may be utilized to define the optimal antibody surface density. Antibodies are quite expensive and minimizing the surface density may have significant cost benefits. Considering only this criteria and the assumption that a crosslinking event must occur to capture an antigen on the immuno-surface, the antibody surface density can be reduced, and significantly reduced for large highly multivalent antigen. To maximize the antibody flexibility while ensuring at least two epitopes are bound within the antigen contact area, the antibody spacing, d_o, must fall within the range $\bar{L} \le d_o \le \sqrt{A_s}$

For spherical antigen, this suggests that the minimum antibody surface density, min R_I, should be dictated by:

$$R_I \ge \frac{1}{A_s N_a} = \frac{1}{\pi\left(\bar{L}^2 + 2\bar{R}\bar{L}\right)N_a}$$

where $\bar{R}$ is the radius of the spherical antigen and $\bar{L}$ is the antibody length, and N_a is Avogadro's number. Fig. 17 provides a comparison between the optimal immuno-surface density predicted maximizing antigen capture with that used to minimize costs and therefore the antibody surface density. The reduced antibody density has a slightly faster lumped antigen

dissociation rate while the amount of antigen bound to the surface during the association phase is dramatically different: the higher the antibody density, the higher the antigen association rate. These effects will become less significant for antigen with lower epitope surface densities or a small size. This demonstrates the tradeoff between cost and performance for the biosensor immuno-surface; for antigen with a lower epitope density, the minimal antibody density may suffice while for highly multivalent antigen the optimal density will perform better.

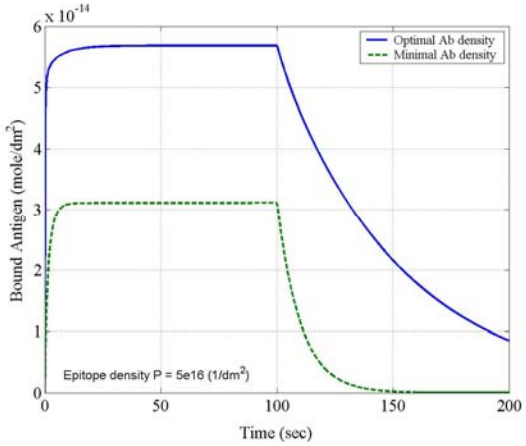

Figure 17: Comparison of the minimal cost and the optimal antibody surface density

2.3.3 The Role of Antibody Attachment and the Immuno-surface Properties - This work confirmed that antigen capture is maximized utilizing high affinity antibodies and also suggested that given a choice for the same antibody affinity: the antibodies with the lower dissociation rate constant will perform better than the ones with higher association rate constant. In the developed model the dissociation rates are constant, k_{-x}, however the association rates are a function of the effective antigen valency, $\nu(i)$. To maximize the effective antigen valency, we want to maximize the antigen contact area, A, the number of epitopes within the antigen contact area, n, the antibody flexibility, φ, and minimize the epitope-antibody contact area, a. As the effects of antibody flexibility were considered in a different section, they are not further investigated here. Instead, the effects of the antigen contact area are explored. The epitope-antibody contact area, a, is not controllable but to some extent the antigen contact area, A, and therefore also the number of epitopes within the antigen contact area, n, is. The surface characteristics can be modified to enlarge the antigen contact surface area. The results shown in Fig. 18 illustrate a relationship between the antigen capture and the antigen contact surface area.

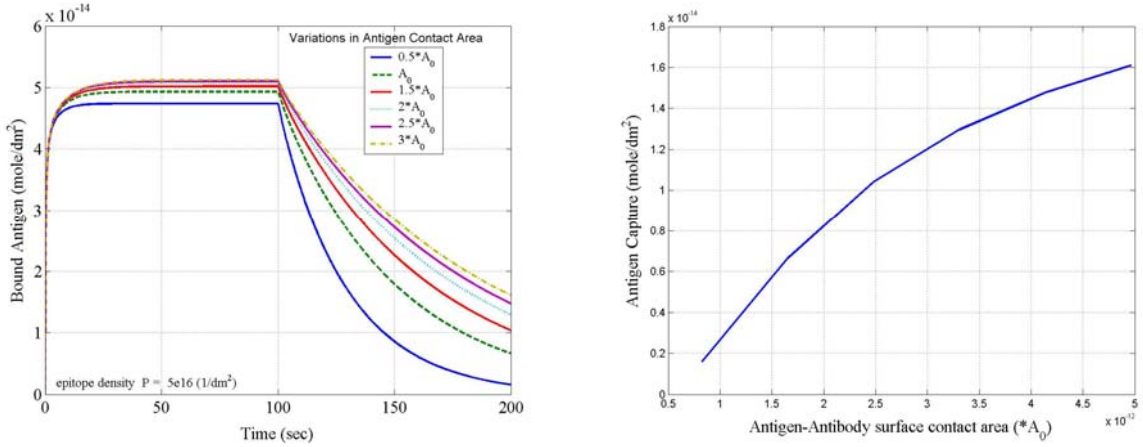

Figure 18: The effects of increased antigen contact area on antigen capture a. Time courses, b. Antigen capture vs antigen contact area

Antigen capture was significantly improved when the antigen contact area was enlarged: the association curves and equilibrium levels are similar for most cases however, significant deviations can be seen in the dissociation waveforms (t>100s). The larger the antigen contact area, the more crosslinking events making it more difficult to dissociate the antigen from the surface.

Not surprisingly the magnitude of this effect is antibody affinity dependent: Fig. 19 compares the antigen capture at 100 seconds after the dissociation starts for antibodies with different association rates. It is apparent from this graph that this effect is most dramatic for the mid range affinity antibodies: antibodies with really low or high association rates were not improved by enlarging the antigen contact area. The moderate range results demonstrate that more low affinity bonds can be as effective as a few high affinity bonds. Interestingly, these types of effects to enhance the antigen contact area are most important for affinities in the range of a naïve B-cell antibody affinity [Roitt et al. 1993] prior to the process of affinity maturation.

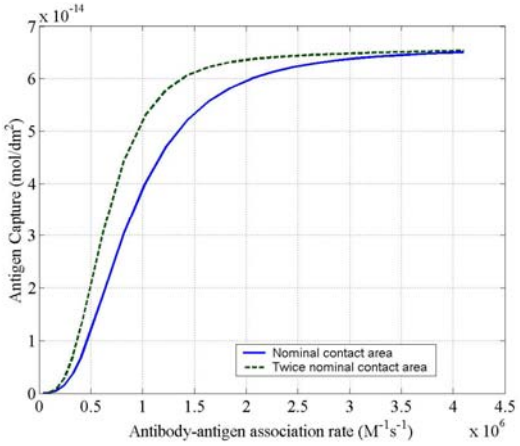

Figure 19: Comparing antigen capture vs. antibody association rate for the nominal antigen contact area and twice the antigen contact area

The antigen contact area, A, is a function of the antibody length and the antigen size and shape. For a spherical antigen

$$A = 2\pi \overline{RL} \frac{\overline{R}}{\overline{R} + \overline{L}}$$

where $\overline{R}$ is the radius of the antigen and $\overline{L}$ is the antibody length. Thus to maximize the antigen contact area, the antibodies should be extended from the surface using linkers such as PEG or a dextran layer. This is analogous to a bowling ball resting on a shag carpet as opposed to a hardwood floor, clearly there is a larger antigen contact area with antibody extensions. The effectiveness of the antibody extensions is a function of antigen size, for small antigen ($\overline{R} << \overline{L}$) this extension has little to no effect while for larger antigen ($\overline{L} << \overline{R}$) the antigen contact area is roughly proportional to the antibody length. The magnitude of this enhancement is still under investigation as our theory predicts for high affinity antibodies this effect is negligible. However, Weimer *et al.* demonstrated significant enhancement of immuno-assays for pathogenic bacteria using antibody PEG linkers [Weimer et al 2000]. These PEG linkers effectively increase the antigen contact area and suggest that the magnitude of the antigen capture enhancement for high affinity antibodies may be under estimated by this method and may be explained as PEG linkers also modify the hydrophilicity of the immuno-surface. Thus future work will investigate the role of surface hydrophilicity on the antigen capture.

Extending the antibody length is not the only means to enhance the antigen contact area. The surface of a B cell is not smooth or rigid: the cell membrane is quite flexible and possesses many features that extend from the surface [Roitt et al 1993]. A flexible or soft substrate, instead of a rigid one, may enhance the antigen contact area: much as a bowling ball resting on a pillow has a larger contact area than when on a hardwood floor.

Yet another alternative approach may use an immuno-surface with surface roughness on the order of the target antigen size. This would increase the antigen contact area, similar to an egg in an egg carton. Experimental evidence supports this type of surface roughness modification in the study of cell attachment; it promotes cell adhesion with nanometer scale surface roughness for hard and soft tissue applications [Webster et al 2001].

2.4 Conclusions to Section 2

Modeling multivalent antigen capture has not been fully resolved: a precise mathematical formulation that reflects and predicts antigen capture has not been elucidated. The model developed herein incorporates multivalent antigen binding based upon the probability of a crosslinking event which is dependent upon the steric hindrances such as relative spacing, orientation, alignment of the antigen epitopes on the antigen contact area, and the immobilized antibodies and their flexibility. In this manner, the model evolved from historical models of crosslinking of cell-surface receptors to include the local and far-field antibody surface density effects, the incorporation of immobilized antibodies, and an accommodation of the flexibility and range of motion of immobilized antibodies.

This work illustrates that the far field antibody surface density impacts the binding dynamics as the surface density drives the rate of initial an antigen association. This is purposefully differentiated from the local antibody surface density that controls the rate of multiple bond formations between the antigen and immobilized antibodies. The far field antibody surface density effects modify the association rates as a function of the available surface area on the immuno-surface whereas the local surface density and the antibody immobilization effects play the largest role in the antigen release from the immuno-surface during the dissociation phase as they limit the number of antibodies bound per antigen at multiple epitopes.

Analyzing the developed model identified potential controllable properties (affinity, surface density, antibody attachment) to enhance the immuno-surface antigen capture capabilities. Naturally occurring antibodies differ most in their dissociation rates; the association rates are quite similar. A higher affinity antibody typically has a lower dissociation rate. Our model demonstrated that this method for achieving a higher antibody affinity maximizes the amount of multivalent antigen captured on the immuno-surface. This suggests that given a choice between antibodies with equivalent affinities, an immuno-based biosensor, which employs a rinse step to remove non-specifically bound antigen, should use the antibodies with the lowest dissociation rate.

Our model of multivalent antigen capture by an immuno-based biosensor is unique in its incorporation of the antibody flexibility. This was accomplished by introducing the concept of a reachable area for immobilized antibodies. The incorporation of the antibody immobilization and flexibility within the model is a function of the antibody surface density and provides a mechanism to explore the impact of different immobilization methods. The simulation results from the model demonstrate that as the antibodies are packed tightly together they interfere with one another and inhibit antigen capture, this is in agreement with experimental qualitative observations. To the best of our knowledge, this is the first time the antibody surface density inhibition has been explored and potentially explained analytically. Interestingly, this result suggests an optimal antibody surface density exists which is independent of the antigen-epitope spacing or density. The mobile antibodies when uniformly distributed on the surface of a B-cell are less densely spaced by a factor of about 5 times the surface density, suggesting that the

immobilization of the antibodies necessitates more antibodies to achieve maximal antigen capture.

Analysis of the model also indicated that maximizing the antigen contact area effectively increases the effective antigen valency and promotes crosslinking. Simulations confirmed that antigen capture was significantly improved when the antigen contact area was enlarged; the larger the antigen contact area, the more crosslinking events making it more difficult to dissociate the antigen from the surface. There were several methods suggested to enlarge the antigen contact area including antibody extensions, immuno-surface flexibility, and immuno-surface roughness. These methods to enlarge the antigen contact area were inspired by properties of the B-cell membrane; its flexibility and nano to micron surface roughness features. These membrane properties may facilitate the antigen-antibody bond formation thereby promoting antigen capture.

In short, a nonlinear differential equation model of multivalent antigen binding to immobilized antibodies has been developed. The dynamics of this model were explored to determine insights for improving immuno-based biosensor performance. Throughout this work, comparisons to B-cell surface antibody and membrane properties were drawn to illustrate and serve as an inspiration for immuno-surface design.

3.0 Impact of Surface Roughness and Energetics on Immuno-surface Functionality

To maximize antigen-antibody capture, the present study designed, synthesized, and evaluated the influence of surface roughness and energetics on immunoassay functionality. Varying degrees of roughness was achieved by immobilizing Protein A conjugated gold particles and Protein A conjugated polystyrene particles that ranged in size from 40 nm to 860 nm. It is hypothesized that a surface roughness, characteristic of B-lymphocyte cell membranes, will promote antigen-antibody interactions and minimize nonspecific binding. To test this hypothesis, this study prepared polystyrene 96 well plate surfaces to have similar topographies as those of B-lymphocyte cell membranes. Atomic force microscope images provide evidence of a well-dispersed immunoassay surface with a high degree of biologically inspired roughness. Results showed that specific antigen capture increased with increased surface roughness and nonspecific antigen capture showed no correlation with surface roughness. This study suggests that surface roughness not only increases the amount of immobilized antibodies, but plays a role in enhancing the functionality of those antibodies on the immunoassay surface. In addition, the surfaces constructed had varying degrees of hydrophilicity. As a result of these studies, it was also found that the more hydrophilic the surface, the more specific antigen capture; while the non-specific antigen capture remained independent of the surface energetics. In this manner, this study provides clues for improving antigen-antibody capture for the design of the next-generation of immuno-sensors/assays. For the Materials and Methods please see Paul Tuttle, "Influence of biologically inspired surface roughness on antigen-antibody interactions", M.S. Thesis, Purdue University, West Lafayette, IN, USA, Dec. 2004, or the soon to be submitted journal article P. Tuttle et. al 2005.

RESULTS AND DISCUSSION
3.1 Characterizing Immuno-Surfaces

3.1.1 Quantifying Surface Roughness with the AFM - The AFM was used to quantify the surface roughness for the various constructions as either conventional or with immobilized 40 nm, 460 nm, and 860 nm particles. The topographical differences can be visualized in the 3D representation of each of the four surface types, see Fig. 20. AFM measurements show that the surface roughness between the conventional polystyrene 96 well plate, 40 nm, 460 nm, and 860 nm particles are statistically different with respect to the RMS roughness, mean roughness (R_a), and change in surface area (Δ SA, 3D surface area / 2D surface area), Fig. 21, regardless of the surface roughness measurement. The surface roughness increases with increasing particle size. The conventional polystyrene surface of the 96 well plate showed small ridges that have been reported by others [Qian et al 2000]. The 40 nm surface displayed spiky features, the 460 nm surface showed oval features, and the 860 nm surface exhibited spherical features. The height of the surfaces increased as the particle size increased as noted with the z-axis. From these images, it can be observed that the topology of the surface depends upon the size of the particle immobilized. Importantly, the particles chosen for these studies clearly span a wide range of interest for these studies.

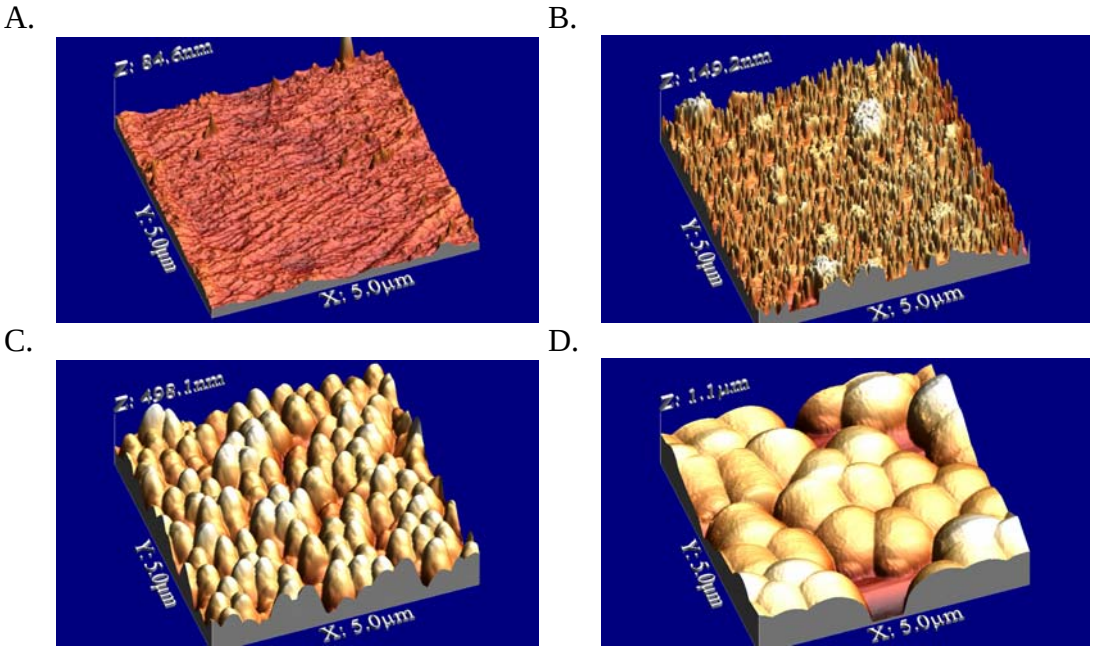

Figure 20: 3D AFM Images of Surfaces: AFM 3D surface images with physisorbed antibody solution concentration of 11.1 µg/mL obtained using tapping mode in air of (A) Conventional 96 well polystyrene plate, (B) Stock 40 nm gold nanoparticles conjugated with Protein A to a 96 well plate, (C) Stock 460 nm polystyrene particles conjugated with Protein A attached to a 96 well plate, and (D) Stock 860 nm polystyrene particles conjugated with Protein A attached to a 96 well plate. Each image is 5 µm by 5 µm scan at a resolution of 512 X 512 with a tip velocity of 10 µm/sec (1 Hz). Engage set point was 0.7 V.

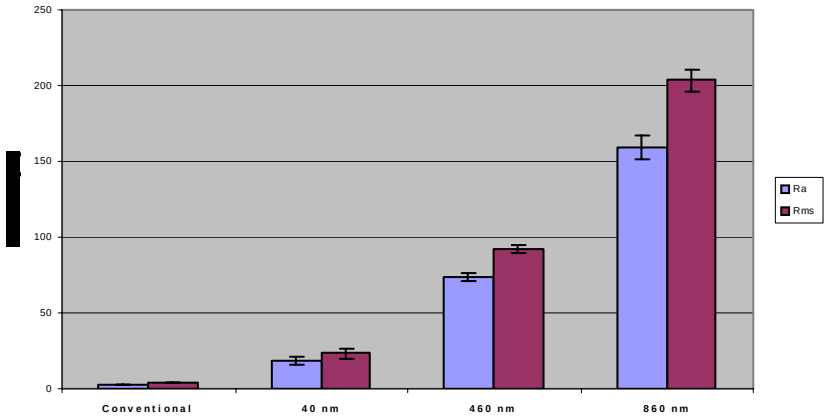

Figure 21: Increasing mean roughness (R_a) and RMS roughness with increasing particle size at the 1:0 particle concentration. Physisorbed antibody solution concentration of 11.1 µg/mL. All surfaces are statistically significantly different from each other within each surface roughness measurement technique with P<0.01. 5 µm x 5 µm scan size. Data = Mean +/- SEM, N=9.

3.1.2 Quantifying Protein A surface densities - Fig. 22 showed that there was more protein A on the 460 nm particle with less surface area than the 860 nm particles. Both the 460 nm and 860 nm particles had more protein A per particle than the 40 nm. Note that the number of IgG binding sites reported by Spherotech per 860 nm particle is 53,000.

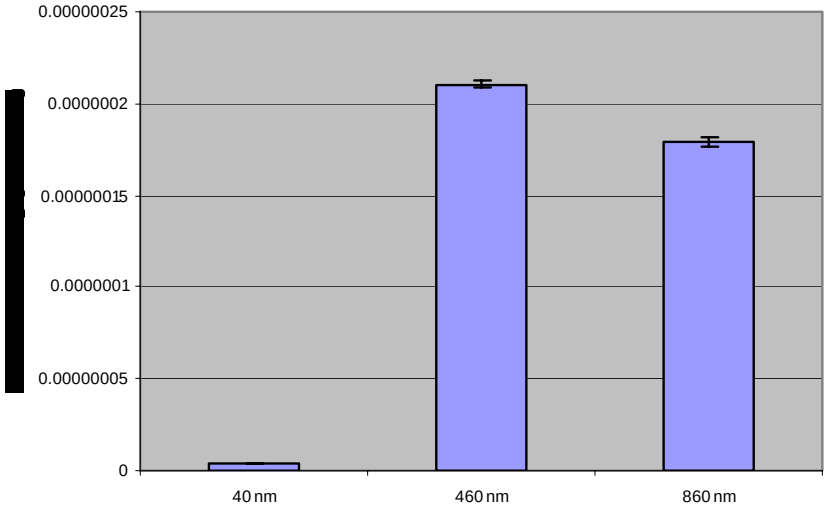

Figure 22: Varying amounts of protein A on particle types as determined using a MicroBCA assay. All surfaces statistically significant to each other with P<0.01. Data = Mean+/- SEM, N=3.

Fig. 23 showed that surface density of protein A on the immuno-surfaces does not necessarily increase with an increase in the size of the particles. These were quantified using the MicroBCA™ assay. Interestingly, the roughest surface did not have the most protein A, since the 460 nm surface had the most protein A. The conventional surface protein A density is far below the 40 nm surface. The conventional immuno-surface protein A density is 0.004146 +/- 0.0022 $\mu g/mm^2$ (Mean +/- SEM).

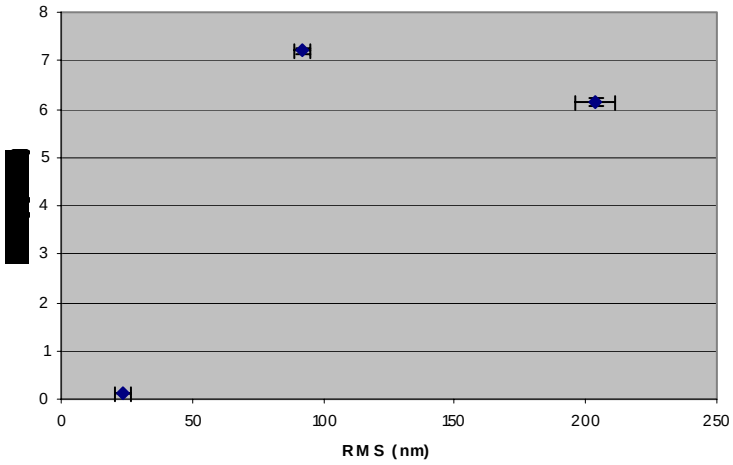

Figure 23: PA surface density does not depend on surface roughness. 40 nm surface type is the left point, 460 nm surface type is the middle point, and 860 nm surface type is the right point. Data = Mean +/- SEM

3.1.3 Quantifying Surface Energetics - Measurements of the hydrophilicity or hydrophobicity were done to determine the surface energy of the substrates by using Young's equation which relates the contact angle and surface tensions of the liquid and solid phases. This data was taken using "Tantec's Half-angle method" with water under static conditions. In Fig. 24, it is observed that there are different surface energetics at certain surface roughness values across various immobilized particle types. For example, at the 100 nm surface roughness regime there is a difference in surface energetics between and within the 860 and 460 nm immobilized particle types. Moreover, within each immobilized particle type the surface energetics change as the surface roughness changes. However, these changes within each surface type happen at different rates between each surface type. The 40 nm surface decreases at the highest rate (-3.9203), the 460 nm surface decreases at an intermediate rate (-0.2542), and the 860 nm surface decreases at the slowest rate (-0.0661). The conventional surface contact angle is 76.67 +/- 3.52 (Mean +/- SEM). From these results, it is apparent that the changes in contact angle were not strictly dependent upon the changes in surface roughness. Thus the surface energy is a function of both topography and composition (surface chemistry). These data characterizing the surface energies will be useful for interpreting the functionality studies for the various surfaces.

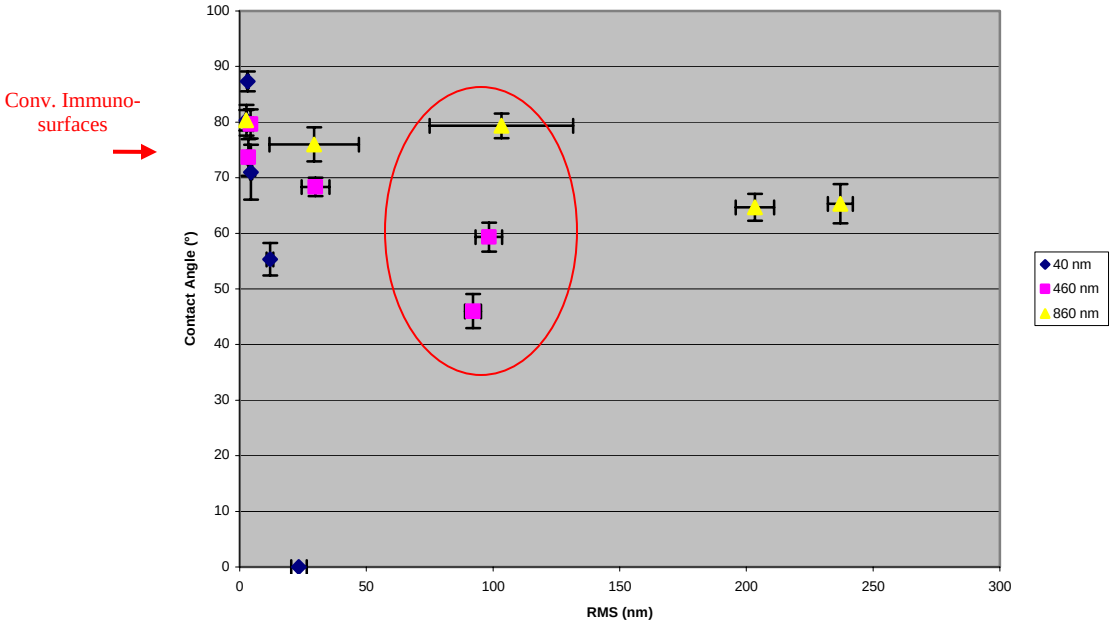

Figure 24: Different surface energetics at various surface roughness values between and within surface types. Circle highlighting possible different surface chemistries at the 100 nm regime. Data = Mean +/- SEM.

3.2 Quantifying Functionality of Immuno-surfaces

3.2.1 Immuno-surface functionality as a function of surface roughness - Each of these different surfaces were tested for their functionality in terms of specific and non-specific antigen capture. Analysis was conducted to determine whether the differences in antigen capture can be attributed to the actual changes in the surface roughness, surface energetics, or simply those resulting from an effective increase in surface density of immobilized antibodies. Fig. 25 suggests that increased surface roughness results in increase specific antigen capture. The change in surface roughness data within each surface type reflects the serial dilutions of the particles (1:0, 1:10, 1:100, 1:1000, and 1:10000). Fig. 26 shows that nonspecific binding is independent of the degree of surface roughness, as there is no observable trend between the two variables. In both Fig. 25 and Fig. 26 there are changing amounts of antigen capture at the 100 nm surface roughness regime. The functionality of the conventional surface (specific antigen capture) in Fig. 25 is 76.13 +/- 21.15 (Mean +/- SEM), and in Fig. 26 the nonspecific antigen capture on the conventional surface is 11.00 +/- 8.11 (Mean +/- SEM).

Fig. 25 suggests that specific antigen capture increased as the surface roughness increased, and Fig. 26 showed that nonspecific antigen capture is independent of surface roughness. Fig. 25 and 26 highlighted that even though surface roughness may play a factor, there are likely other factors involved such as a change in surface chemistry or protein A density. This is likely since at the 100 nm regime there is a difference in specific and nonspecific antigen capture. This can further be confirmed in Fig. 24 where at the 100 nm regime the surface types have different surface energetics. This may be due to a change in surface chemistry from the different types of polystyrene particles used and/or the different amounts of protein A on those particles as seen in Fig. 22.

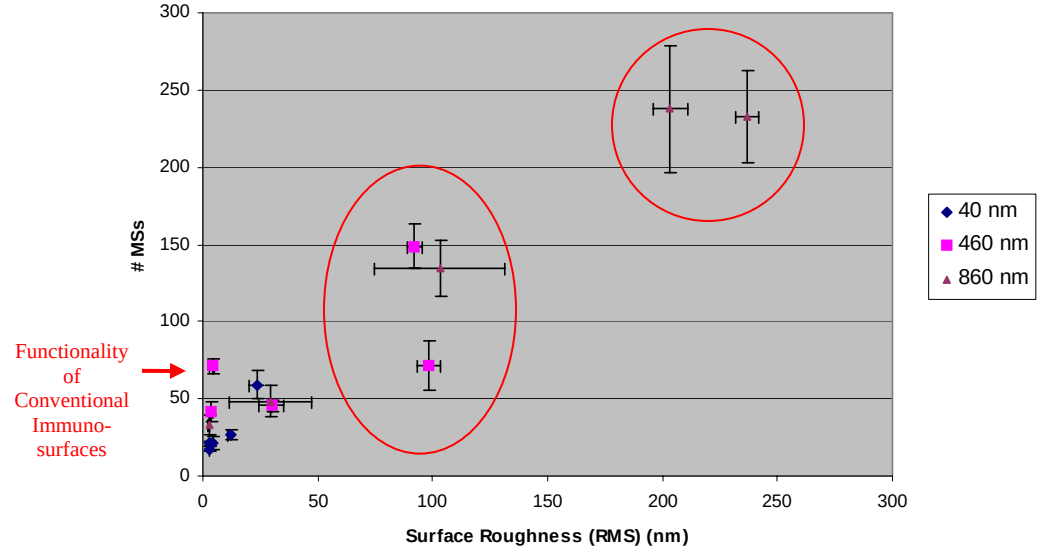

Figure 25: Increased specific antigen capture with increased degree of immobilized particle size as a function of surface roughness. The circles are highlighting the changing specific antigen capture at the 100 nm regime, and the statistical increase in specific antigen capture with increasing surface roughness. Data = Mean +/- SEM.

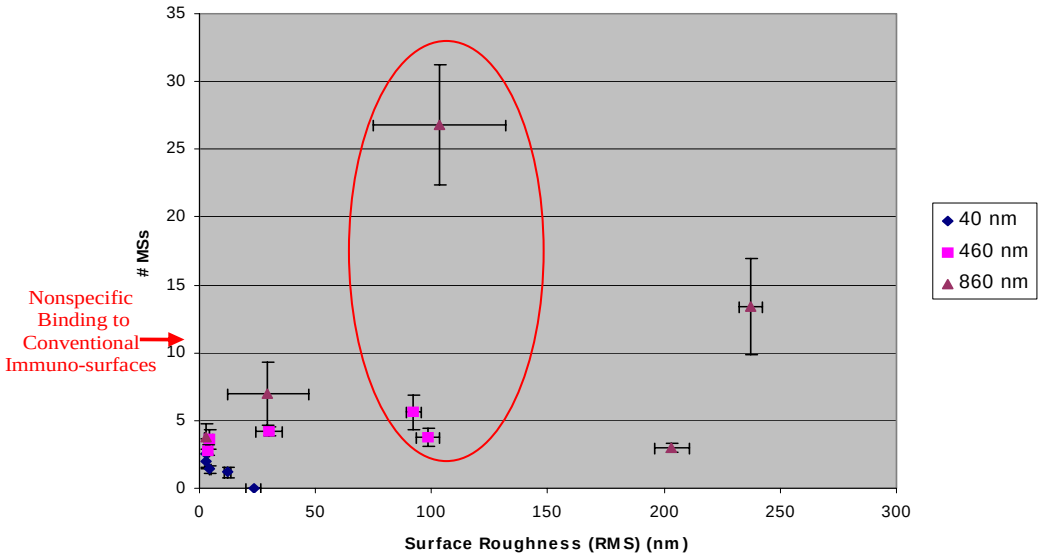

Figure 26: Non-specific binding independent of degree of surface roughness. The circle is highlighting the changing nonspecific antigen capture at the 100 nm regime. Data = Mean +/- SEM.

3.2.2 Immuno-surface functionality as a function of surface energetics - Fig. 27 showed that there was a trend between specific antigen capture and surface energetics. Within all surface types, the more hydrophilic the surface the more specific antigen capture occurred. Fig. 28 showed that there was no trend between nonspecific antigen capture and surface energetics. In both Fig. 27 and Fig. 28, surfaces that had similar surface energetics showed different amounts of specific and nonspecific antigen capture.

Fig. 27 showed that as the 860 and 460 nm surfaces became more hydrophilic, they exhibited higher amounts of specific antigen capture. This is most likely due to the polar nature of the DNP antigen. The more charged or the more hydrophilic a surface becomes, the more likely it will attract a charged molecule such as DNP. Fig. 27 and 28 both highlight that specific and nonspecific antigen capture change when the surface energetics are held constant. These two graphs are complement to the previous three graphs since they show that when either surface roughness or surface energetics are held constant, there still is a change in specific and nonspecific antigen capture. That is, specific and nonspecific antigen capture is most likely due to a combination of a change in surface chemistry and surface roughness.

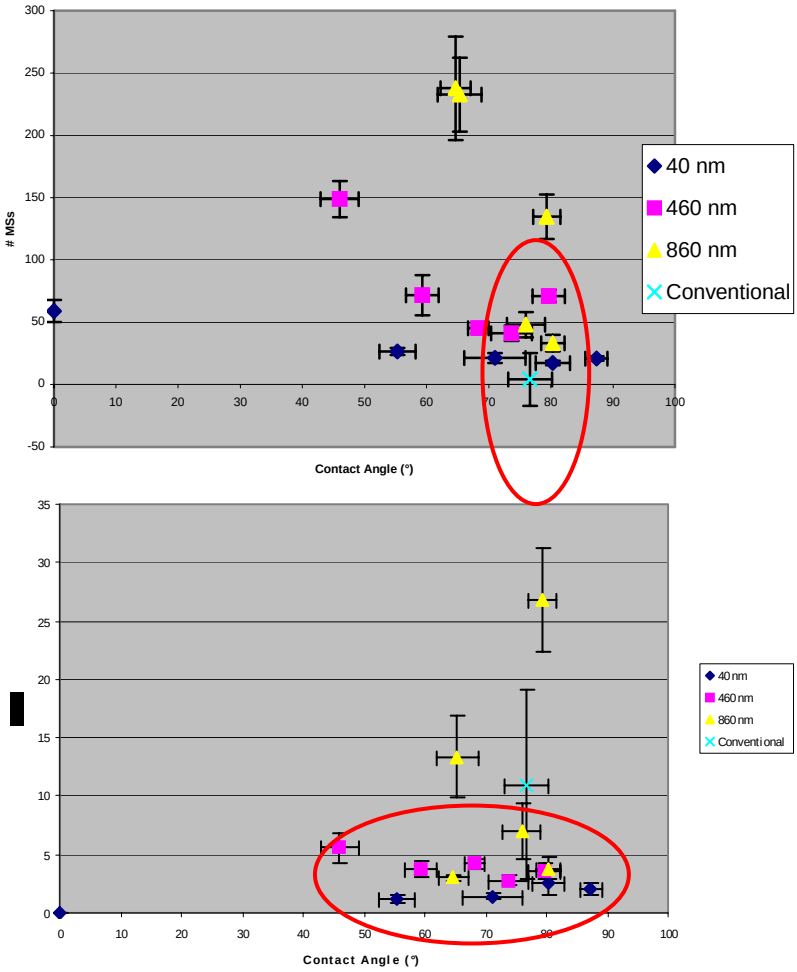

Figure 27: Varying specific antigen capture with equal surface energetics over various surface types. Circle highlighting changing specific antigen capture without a significant change in surface energetics. Data = Mean +/- SEM.

Figure 28: Varying nonspecific antigen capture with equal surface energetics over various surface types. Circle highlighting change in surface energetics without a significant change in the nonspecific antigen capture. Data = Mean +/- SEM.

3.2.3 Immuno-surface functionality as a function of protein surface density - Fig. 29 and Fig. 30 showed that specific and nonspecific antigen capture does not dependent on the density of protein A on the surface. The same protein A density corresponded to varying amounts of specific and nonspecific antigen capture.

Fig. 23 showed that the density of protein A does not correlate to surface roughness. This suggests that surface roughness does not correlate to surface energetics, since the amount of hydrophilic protein A on the hydrophobic polystyrene will change the energetics of the surfaces depending on what particles are tested and the concentration of those particles on the hydrophobic polystyrene 96 well plate. Figs. 29 and 30 showed that when the protein A density was held constant there was once again a change in specific and nonspecific antigen capture, respectively. This suggests that the change in surface chemistry is also a function of the underlying particle material, in addition to the amount of protein A on that particle and the number of particles on the surface. In Fig. 31 the disproportionate increases in specific antigen capture with respect to physisorbed antibody solution concentrations suggests that the increase in specific antigen capture may be due to an increase in the amount of antibody immobilization and/or an increase in the functionality of those antibodies that are immobilized on the immunosurface. This highlights the possibility that it may not just be the amount of IgG adsorbed but the functionality of those adsorbed antibodies, since the most specific binding was not found on the surface with the most protein A.

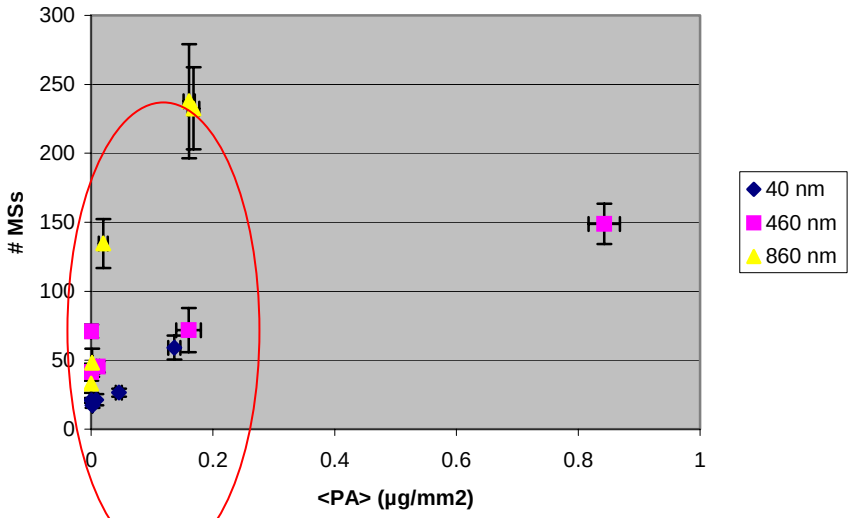

Figure 29: Specific antigen capture does not depend on protein A surface density. Circle highlighting changing specific antigen capture without a change in protein A density. Data = Mean +/- SEM.

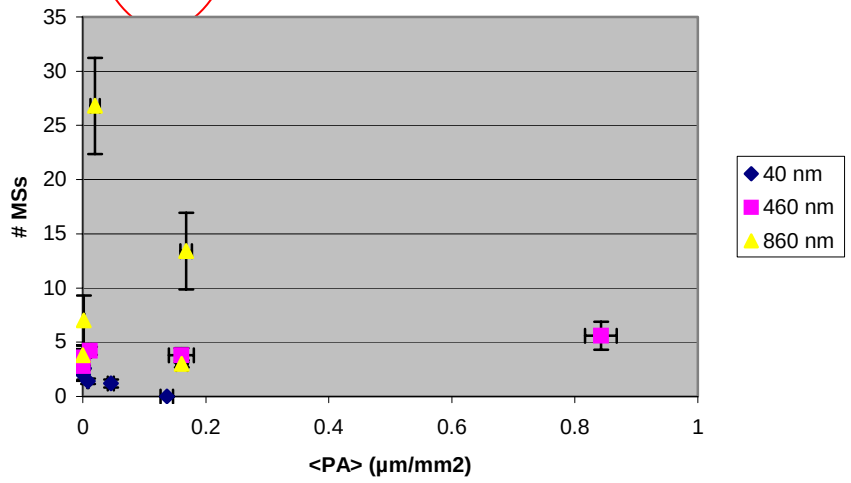

Figure 30: Nonspecific antigen capture does not depend on protein A surface density. Circle highlighting changing nonspecific antigen capture without a change in protein A density. Data = Mean +/- SEM.

Fig. 31 showed increasing specific antigen capture with respect to an increasing RMS surface roughness at increasing physisorbed antibody solution concentrations. A disproportionate increase in specific antigen capture was seen with respect to increased surface roughness and physisorbed antibody solution concentration. Specific antigen capture at 11.1 µg/mL increased by approximately 540% while the surface roughness increased by approximately 1900%.

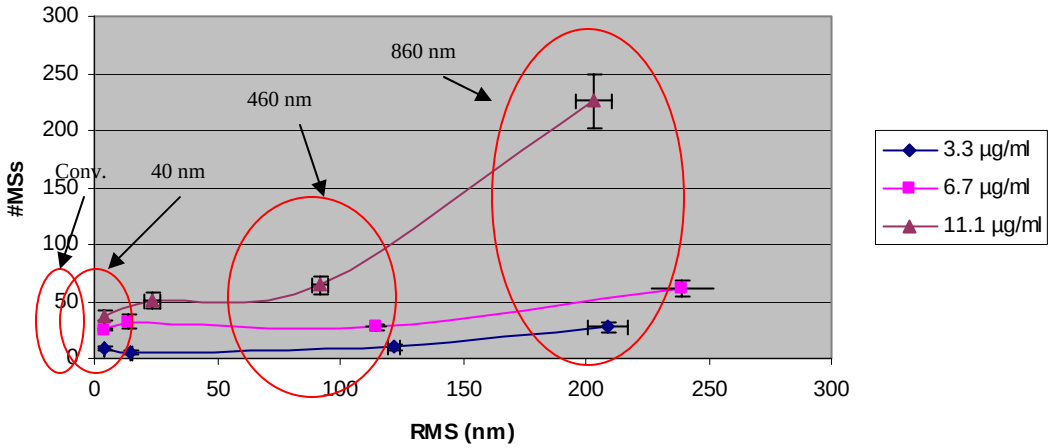

Figure 31: Increasing specific antigen capture with increasing surface roughness (RMS) and increasing physisorbed antibody solution concentrations. Surface types are at stock (1:0) levels. Circles represent different surface types across physisorbed antibody solution concentrations. Data = Mean +/- SEM.

3.3 Conclusions to Section 3

Biologically inspired surface roughness has been shown to most likely enhance specific antigen capture while leaving nonspecific antigen capture independent of surface roughness. This surface parameter would improve the sensitivity and efficacy of present day immuno-sensors/assays within the fields of healthcare, food safety, environmental monitoring, and national defense. When surface roughness and surface chemistry are both changing it is difficult to determine which variable is contributing more to the change in specific and nonspecific antigen capture. However, these results show that surface roughness is very likely an important parameter. Moreover, the largest specific antigen capture was seen at 860 nm which corresponds closest to the estimated surface roughness from the image of the B-lymphocyte in Fig. 32. The change in surface area has been calculated to be 1.851431 +/- 0.034405 (Mean +/- SEM). This roughness value is rougher but closest to the 860 nm surface type.

In conclusion, this study has further suggested that surface roughness and surface energetics may be critical factors in designing future immuno-sensors/surfaces, since the sensitivity may be enhanced without an increase in false positives from nonspecific binding.

An increase in surface roughness was seen with an increase in size of the immobilized particles, and a decrease in surface roughness was seen through the serial dilutions of those immobilized particles. An increase in specific antigen capture was seen to correlate with an increase in surface roughness and physisorbed antibody solution concentrations, while

nonspecific antigen capture was independent of surface roughness. Surface energetics experiments suggest that there may be a change in surface chemistry between the different surface types. However, even amidst a possible surface chemistry change surface roughness may be the dominating factor that contributes to the increase in specific antigen capture.

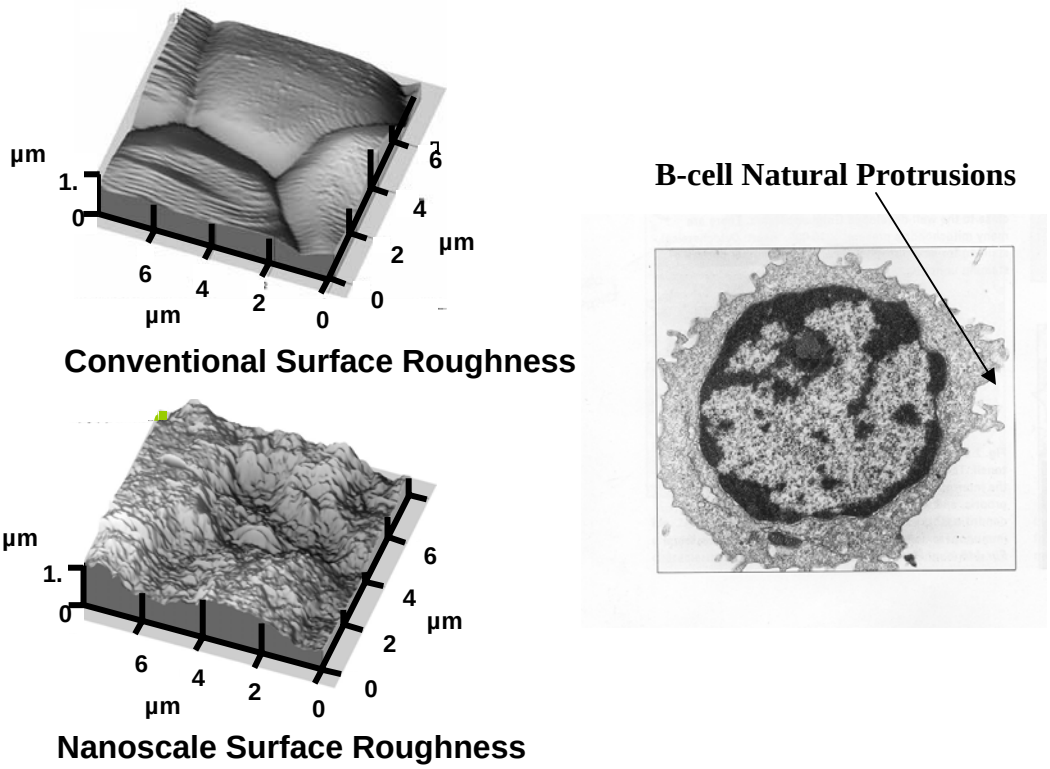

Figure 32: Surface Roughness Comparison. (Left) Topography difference between nanoscale and conventional surfaces (Adapted from [Ying 2001]); (Right) B-lymphocyte surface roughness, 10-15 µm in diameter (Adapted from [Roitt et al. 1993]).

4.0 A Modeling Study of the Effect of Protein Mobility on Functionality

Two mathematical models were created to quantitatively evaluate the effects of antibody and epitope diffusion on antigen capture.

4.1 Considering antibody diffusion

MODEL DEVELOPMENT

Antibodies on the surface of B-cells are mobile and are not rigidly held in place. This mathematical model will help estimate the importance of this characteristic of antibodies on B cells, antibody mobility, to antigen capture for biosensors. To make this problem tractable, only a single antigen was considered and the epitope locations on the antigen are initially assumed to be rigidly held in place, see Fig. 33. The antibodies are diffusible and will diffuse to eliminate a gradient in the surface density of free antibodies. Once bound, the antibodies do not move (unless they dissociate from the antigen epitope).

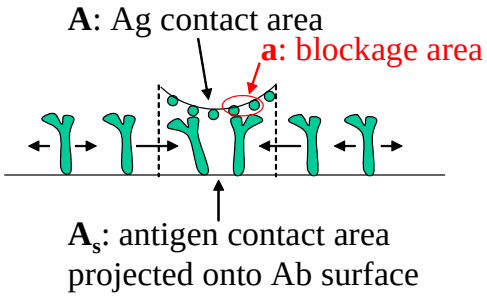

Figure 33: Schematic of antigen binding and diffusion of mobile antibodies on the immuno-surface

The mathematical model, provided in Figure 34, is comprised of partial differential equations which accommodate both temporal and spatial variations. The independent model variables are the bound antigen epitope density, $x_b(t,\lambda)$ also equivalent to the bound antibody density, and free antibody density, $R_f(t,\lambda)$. The effects of steric hindrances, explored previously in more detail, are incorporated through the probabilistic rate modification term indicated in the figure. The Laplacian operator in the free antibody density equation ensures diffusion of the free antibodies into regions where the antibodies have been bound by epitopes and hence are at a lower surface density.

Equations:

Probability of a free epitope to be accessible to antibodies:

(N_a: Avogadro's number)

k_x: crosslinking association rate

k_{-x}: crosslinking dissociation rate

D: diffusion coefficient

Bound antigen epitope/ antibody density:
$$\frac{\partial x_b}{\partial t} = k_x\left(1-\frac{x_b A_s N_a a}{A}\right)x_f R_f - k_{-x}x_b$$

Free antigen epitope density:
$$\frac{\partial x_f}{\partial t} = -\frac{\partial x_b}{\partial t}$$

Free antibody density:
$$\frac{\partial R_f}{\partial t} = D\nabla^2 R_f - \frac{\partial x_b}{\partial t}$$

Boundary condition:
$$R_f(t,0) = R_f(t,L) = R_0 \quad \text{(assume 1-D space)}$$

Figure 34: Partial differential equations incorporating antibody diffusion with epitope binding

RESULTS AND DISCUSSION

Fig. 35 indicates the spatial distribution of the bound (green curve) and free (blue curve) antibodies along a one dimensional strip of length $1e^{-11}$dm for different diffusion rates. When the antibodies are not diffusible (as shown in Fig. 35a) only the antibodies within a reachable distance are bound to the antigen. These antibodies bind uniformly across the entire antigen contact area because we assume uniform distribution of the epitopes and antibodies. For the case of moderate diffusion rates (Fig. 35b), there is more binding at the edges as the free antibodies diffuse into the antigen contact area and bind immediately to the available epitopes at the edges of the contact zone. Eventually, the antibodies will diffuse into the center of the contact zone, it just takes longer but with higher diffusion rates this happens quicker. In Fig. 35 the maximal difference in the distribution of free antibody surface density (maximum curvature in the blue lines with time) are plotted. These are not necessarily at equilibrium yet.

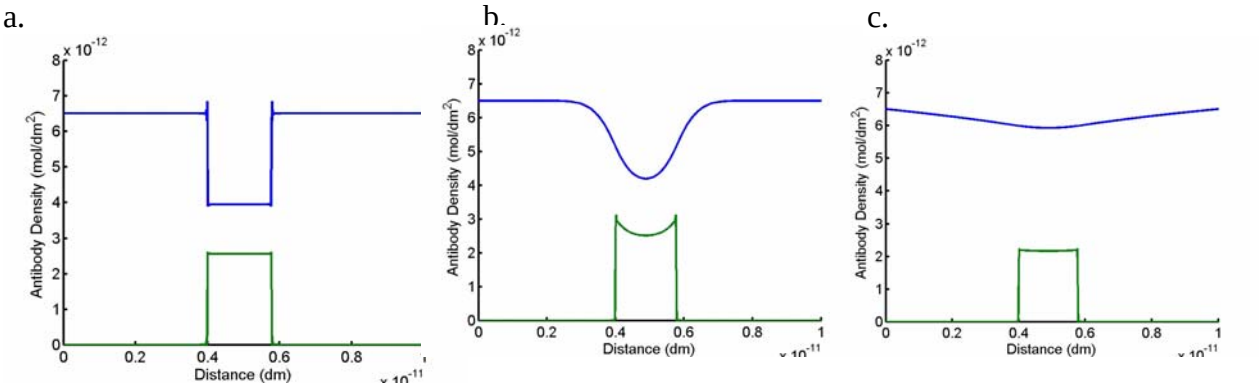

Figure 35: Snapshot of The Maximal Deviation in the Density Distribution of Free vs. Bound Antibody: a. D = 0 dm^2/s, b. D = $1e^{-26}$ dm^2/s, c. D = $1e^{-24}$ dm^2/s

To quantify these observations for a comparison of the effects of diffusion on antigen capture, the time course of antigen epitope binding is provided in Fig. 36 for different antibody diffusion rates. From this curve it is more obvious that an increase in the mobility of the antibodies promotes more epitope binding per antigen. However, the improvement in the epitope binding saturates with increased antibody mobility and will not exceed that shown for D = 1 dm^2/s.

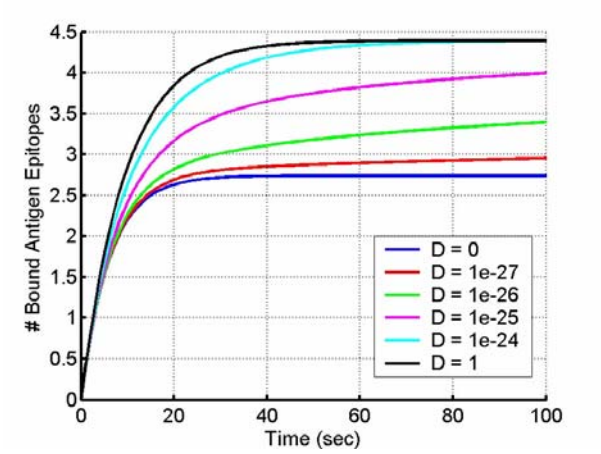

Figure 36: Dependence of Epitope Binding on Antibody Mobility (the units of D are dm^2/s)

To understand the significance of this change in epitope binding, a computational study was completed to determine how this improvement changes with antibody receptor surface density.

These results are shown in Fig. 37a where Δ is the maximum potential fractional enhancement with fully diffusible antibodies (D = 1 dm^2/s). From this figure, it is clear that it is clearly beneficial to have mobile receptors when the surface density is low, however, for higher surface densities of antibodies, the benefits of mobility decrease and approach 10%. For a comparison, the antibody surface density on a typical B cell is roughly 5.3e-12 mol/dm^2 assuming 1e5 BCR/cell and a cell diameter of 10micron and thus the mobility of its receptors significantly contributes (>60%) to its ability to capture antigen. Fig. 37b indicates how Δ changes with antigen epitope density. Although the epitope density is not a characteristic that is easily modifiable for biosensor development, it is interesting to note that high epitope surface densities substantially can improve the number of bound epitopes per antigen by nearly nine times. This curve saturates as the antibodies cannot pack more densely.

a. b.

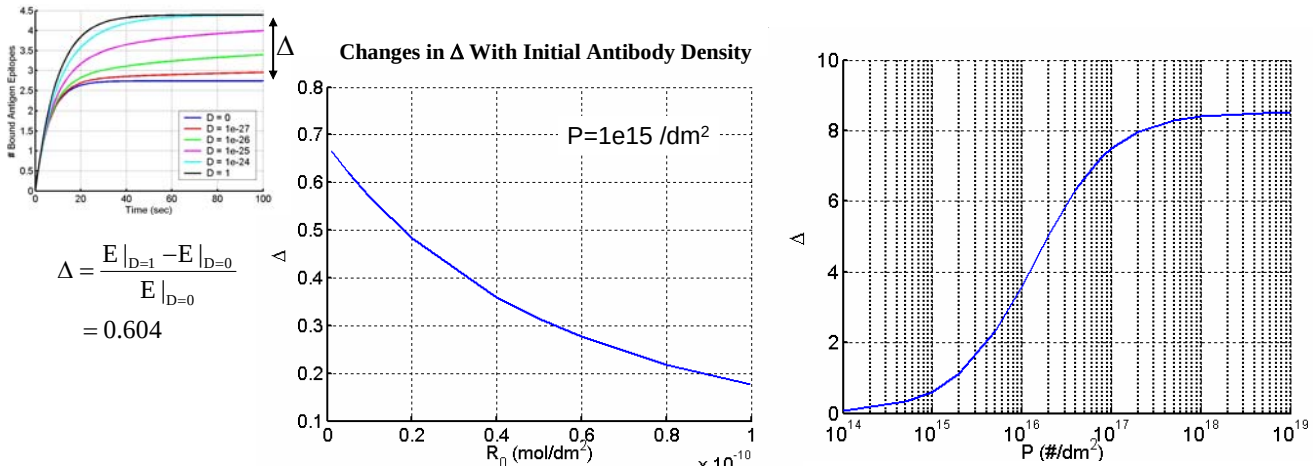

Figure 37: Quantifying Impact of Antibody Mobility Changes in Δ With: a. Different Antibody Surface Densities, b. Different Antigen Epitope Surface Densities with the antibodies at 6.5e-12 mol/dm^2

Fig. 38 considers the relationship of the association and dissociation rates with the mobility of the antibodies. Not surprisingly in Fig. 38a, for rapidly dissociating antibodies (lower affinity) the mobility does not improve the number of bound epitopes. While for slow dissociation processes (higher affinity), the mobility significantly increases the number of epitopes bound per antigen. Thus, this indicates that non-specific binding should not increase with the mobility of antibodies however, the mobility does not reduce the influence of non-specific binding. Figure 38b indicates how for antibodies of the same affinity, there can be slight differences in the binding efficiencies depending upon the association or dissociation rate constants (their ratio being held constant). Comparing more slowly dissociating antibodies with rapidly dissociating ones, the improvement is minimal (< twice of antigen capture at $k_d = 0.01s^{-1}$). Interestingly there is no improvement in capture with the decreased dissociation rates.

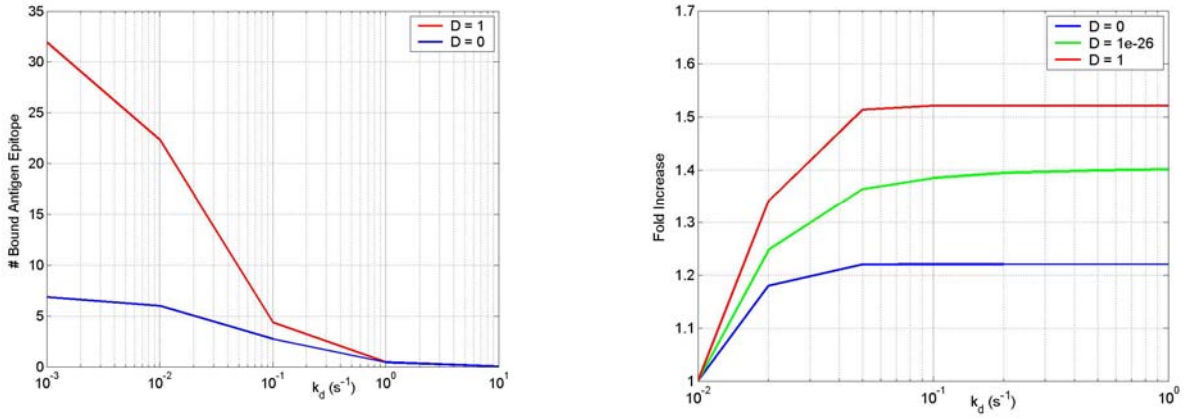

a b

Figure 38: Exploring Antigen Epitope Capture by Mobile Antibodies: a. the association rate, k_a is fixed at 4.1e7 dm^2/mol/s, and the dissociation rate, k_d, is changed, b. the antibody affinity is held constant (the ratio of the association to dissociation rate was 4.1e8 dm^2/mol)

4.2 Considering epitope diffusion

MODEL DEVELOPMENT

This model is developed to investigate the relationship between antigen epitope and antibody mobility on the efficiency of antigen epitope capturing by immuno-surface. Based on the previous model (from Section 4.1), this model takes into account the mobility of both antibody and antigen epitopes. Both free and bound antigen epitopes diffuse in response to density gradient. The antibodies and epitopes have separate diffusion coefficient depend on the nature of the surfaces that support them. The diffusion coefficient of the bound antibody or epitope is lower than that of the unbound antibody or epitope as both the engaged antibody and epitope need to move together. The model is formulated as follows:

x_b: surface density of antigen epitope bound to an antibody

x_f: surface density of free antigen epitope

R_f: surface density of unbound antibodies

$$\frac{\partial x_b}{\partial t} = \min(D_R, D_x)\nabla^2 x_b + k_x(1-\frac{x_b A_g N_a a}{A})x_f R_f - k_{-x}x_b$$

$$\frac{\partial x_f}{\partial t} = D_x\nabla^2 x_f - k_x(1-\frac{x_b A_g N_a a}{A})x_f R_f + k_{-x}x_b$$

$$\frac{\partial R_f}{\partial t} = D_R\nabla^2 R_f - k_x(1-\frac{x_b A_g N_a a}{A})x_f R_f + k_{-x}x_b$$

Boundary conditions: $\begin{cases} R_f(t,0) = R_f(t,l) = R_0 \\ \dfrac{\partial x_b(t,0)}{\partial t} = \dfrac{\partial x_b(t,l)}{\partial t} = 0 \\ \dfrac{\partial x_f(t,0)}{\partial t} = \dfrac{\partial x_f(t,l)}{\partial t} = 0 \end{cases}$ Initial conditions: $\begin{cases} R_f(0,x) = R_0 \\ x_f(0,x) = P_0 \\ x_b(0,x) = 0 \end{cases}$,

where D_R and D_x are the antibody and epitope diffusion coefficient, respectively, R_0 and P_0 are the initial antibody and epitope densities, which are both uniformly distributed over the antigen contact region ([0,l] assuming 1-D space). (It is assumed that the bound antibody-epitope pair diffusion coefficient is the minimum of that of the free epitopes or antibodies.)

RESULTS AND DISCUSSION

4.2.1 Effect of epitope diffusion on the spatial distribution of bound antibodies - Fig. 39 illustrates the effect of diffusible antigen epitopes and antibodies on the surface density of bound epitope-antibody pairs along a one dimensional strip of length 1.765e-12 dm for different antigen epitope diffusion rates. When the antigen epitopes are not diffusible ($D_x = 0$) the epitopes within a reachable distance are bound to the antibodies. Upon binding to the epitopes, a gradient of the free antibody surface density is created within the contact area pointing to its center. This drives new antibodies to constantly flow in across the boundaries, resulting in a relatively higher binding on the boundaries than the center. As the epitope diffusion coefficient is increased to that matching the antibody diffusion coefficient ($D_x = D_R$ = 1e-26dm^2/s) the rapid movement of bound antibody/epitope flattens its density distribution within the contact region.

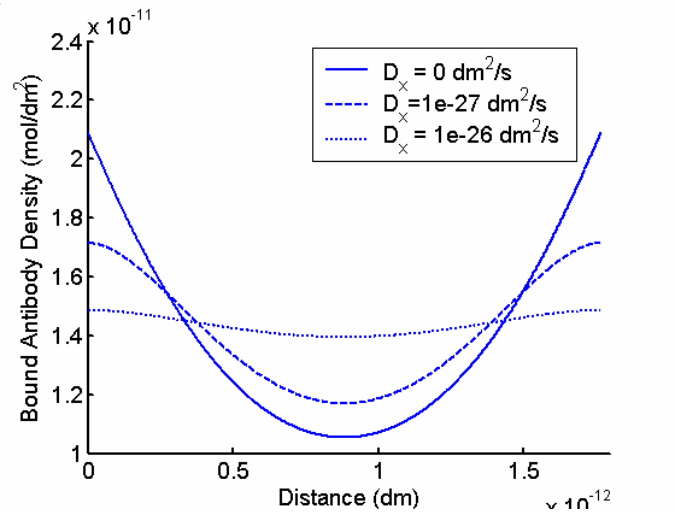

Figure 39: Snapshot of the density distribution of bound Antibody at 100 sec after antigen exposure. D_R = 1e-26 dm^2/s, k_x = 4.1e7 /Ms, k_{-x} = 0.01 /s, P = 1e15 #/dm^2.

4.2.2 Effect of epitope diffusion on the amount of epitope capture - The relationship between epitope capture and its diffusion coefficient D_x turns out to be non-monotonic as illustrated in Fig. 40. At low $D_{x\,x}$ above certain threshold (>1e-30dm^2/s), an increase in the epitope mobility (albeit low) allows the redistribution of both the bound and free epitopes according to density gradient. Therefore, it decreases the spatial constraint on the kinetics of antibody-antigen interaction and allows more epitopes to be bound. When D_x becomes large enough, the movement of the epitope is no longer a limiting factor on the spatial distribution of bound epitopes, causing the total epitope capture come to a plateau. Nevertheless, if the free epitopes move too fast, it creates an additional driving force for the detachment of epitope from being bound to the antibody. This then leads to a slight decrease in epitope capture after the plateau.

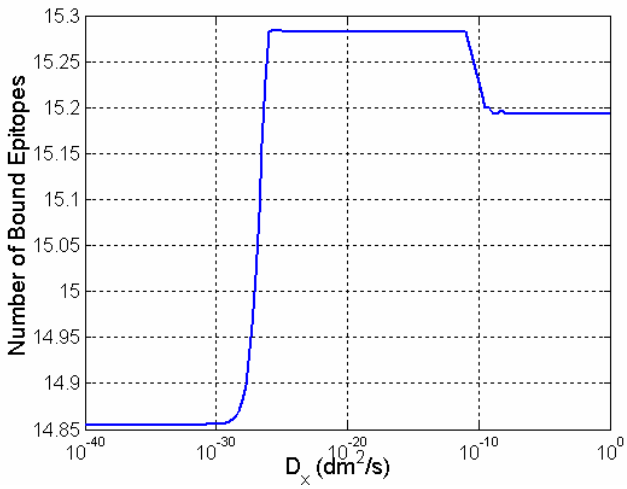

Figure 40: Total number of bound epitopes within the antigen contact area at 100 sec as a function of D_x. D_R is fixed at 1e-26 dm^2/s, k_x, k_{-x} and P are the same as Fig. 39.

4.2.3 Impact from epitope diffusion at different levels of antibody mobility - Fig. 41 compares the relationship between epitope capture (total number of bound epitopes within the antigen contact area at 100 sec) and epitope mobility (D_x) at different values of antibody mobility (D_R). The figure demonstrates that the plateau is always obtained around D_x=D_R. Since the mobility of the bound antigen epitope is constrained by the lower one the two diffusion coefficients, increase in D_x above D_R will not help much in redistributing molecules within the contact area.

Fig. 41 suggests that at different values of D_R, the impact of D_x on epitope capture is not identical. Therefore, to investigate how the impact from epitope mobility changes with antibody mobility, Fig. 42 plots the fractional decrease in epitope capture from $D_x = D_R$ to $D_x = 0$ as a function of D_R. The figure demonstrates that at a certain antibody mobility level between D_R = 1e-27 and 1e-26 dm^2/s, the impact from antigen epitope mobility reaches a maximum. This is anticipated as at low D_R values epitope capture is limited by antibody mobility, while high D_R allows the bound antibody to redistribute in the contact rapidly without the requirement for epitope mobility. Note that at any D_R, the impact from D_x is no bigger than 5%, indicating in general the requirement for antigen epitope mobility is less critical compared to that for antibody mobility.

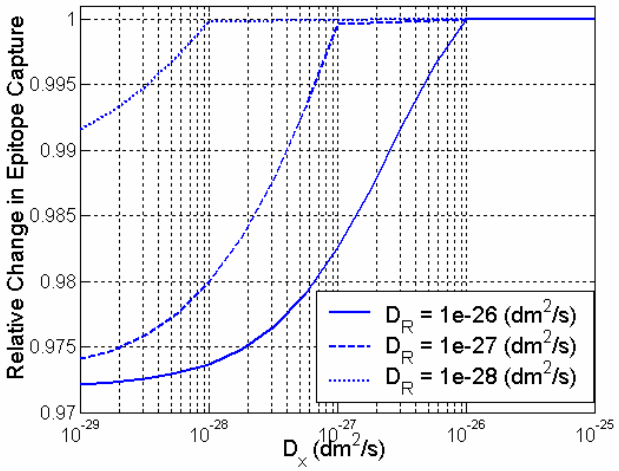

Figure 41: The relative change of epitope capture with varying D_x at different D_R values. Relative change is calculated by diving the actual number of bound epitopes by maximum number of bound epitopes. k_x, k_{-x} and P are the same as Fig. 39.

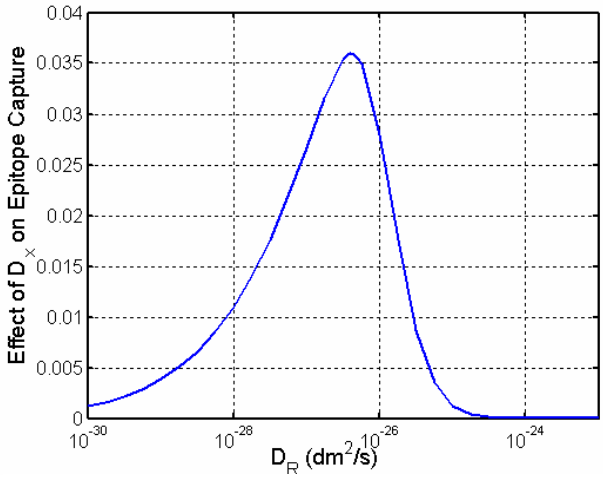

Figure 42: The effect of epitope diffusion changes with antibody mobility. The effect of D_x on epitope capture is calculated as the fractional decrease in epitope capture from $D_x = D_R$ to $D_x = 0$. k_x, k_{-x} and P are the same as Fig. 39.

4.3 Conclusions to Section 4

These modeling and simulation studies suggest that the mobility of the antibodies and the antigenic epitopes may influence the antigen capture functionality. It was found that an increase in the mobility of the antibodies promotes epitope binding. However, for rapidly dissociating antibodies (lower affinity) the antibody mobility does not improve the number of bound epitopes. While for slow dissociation processes (higher affinity), the mobility significantly increases the number of epitopes bound. Thus, this suggests that non-specific binding should not increase with the mobility of antibodies. It was also found that the mobility of the antigen epitope is less critical when compared to that for antibody. In addition, it is beneficial to have mobile receptors when the surface density is low. For higher surface densities of antibodies, the benefits of mobility decrease. It is interesting to note that these studies suggest that the mobility of the antibodies presented on the surface of typical B cell significantly contributes to its ability to capture antigen.

5.0 Recommended Future Research Directions

This work has shown that the immuno-surface with the highest functional antibody density exhibits the greatest specific antigen capture and limits non-specific binding of antigen to the surface. For example, the GMBS method immobilized the greatest amount of antibody and possessed the lowest non-specific binding, while the aminophase surfaces, which orient antibodies, captured the greatest amount of antigen per antibody. These observations illustrate the importance of antibody density and retention of antibody function as they are immobilized. Ideally, future immuno-surface designs should include a surface chemistry motif in which high antibody density and maximum antibody function are achieved to increase biosensor sensitivity. Here it was shown that protein A can increase antibody function on GMBS surfaces, which possess high antibody density, by improving antibody orientation; however, detection methods such as surface plasmon resonance are limited in sensitivity to detect antigen if the antibodies are located relatively far from the surface; this limits the use of protein A. As an alternative, a crosslinker possessing a chemical ring structure similar to that of GMBS could be designed in which the terminal end possessed an amine group similar to the aminophase scheme. By combining the high antibody density characteristic of GMBS with the aminophase method's ability to orient antibodies, this custom-designed crosslinker could possibly achieve high antibody density and function simultaneously, thereby increasing biosensor sensitivity while limiting the distance between the antibodies and the sensor surface. Additionally, covalent immobilization adds stability to the immuno-surface design by decreasing the probability of antibody desorption.

Aside from the immobilization methods, the choice of substrate material may prove invaluable in limiting the non-specific binding of antigen to immuno-surfaces. Investigating hydrophobic surfaces such as polymers may further improve the sensitivity of the immuno-surface for antigen by limiting charge interactions between antigen and the surface and, therefore, decreasing the non-specific binding at the surface. With new innovations, such as the ability to design and build custom chemical crosslinkers and the ability to create custom materials with the ideal properties conducive to immuno-surface functionality, the future of immuno-surface based biosensors is bright.

Biologically inspired surface roughness has been shown to most likely enhance specific antigen capture while leaving nonspecific antigen capture independent of surface roughness. Herein, an increase in surface roughness was obtained with an increase in size of the immobilized particles, while serial dilutions of these immobilized particles caused a decrease in surface roughness. An increase in specific antigen capture correlated with an increase in surface roughness and physisorbed antibody solution concentrations, while nonspecific antigen capture was independent of surface roughness. However, our surface energetics experiments suggest that there may be a change in surface chemistry between the different surface types. Thus future studies should be conducted to isolate and distinguish between the effects of the change in surface chemistry and surface roughness on the specific and non-specific antigen capture. This could be accomplished in a number of manners. A simple extension of this work would be to coat the prepared immuno-surfaces of varying degrees of surface roughness with a thin coat of gold. In this manner, the surface chemistry would be independent of the degree of surface roughness and studies could be conducted to isolate the effects of surface roughness.

The mathematical model developed herein provided significant insight into the antigen- antibody binding dynamics and the role of many of the immuno-surface properties in enhancing antigen capture. These results were achieved with a fairly macroscale model of the process making reasonable assumptions and simplifications to make the problem more tractable. At this point in time and as the immuno-surface properties become more highly characterized, it will become possible to create a mathematical model of the intermolecular surface forces that participate in specific and non-specific antigen capture. Future mathematical models should be derived from first principles of physics and chemistry and address the short and long range molecular forces at work. The mathematical model should consider both the long range forces that play a role in getting the antigen close enough to the immuno-surface to potentially interact as well as the short range molecular forces that predominate in chemical reactions at the atom and molecular scale such as those evident when the antigen binds to the antibody. (The long range forces include van der Waals, steric interactions, and electric double layer forces. The short range forces are primarily electrostatic in origin.) To be useful for specifying immuno-surface properties at the surface chemistry and roughness scales to enhance antigen capture, the mathematical model must be multi-scale in both time and length. That is, it will need to consider both dynamic and equilibrium time scales as well as molecular dynamics and larger environmental forces such as fluid flow and sensor architecture.

6.0 Publications Resulting from this Project

Journal

R. Danczyk, B. Krieder, A. North, T. Webster, H. HogenEsch, and A. Rundell “Comparison of the Functionality of Antibody Immobilization Methods”, Biotechnology and Bioengineering, 84:215-223, 2003.

Y. Zheng, A. Rundell, “Biosensor Immuno-surface Engineering Inspired by B-cell Membrane Bound Antibodies: Modeling and Analysis of Multivalent Antigen Capture by Immobilized Antibodies”, *IEEE Transactions on NanoBioscience*, v 2, n 1, pp 14- 25, Mar 2003.

P. Tuttle IV, T. Webster, A. Rundell, “Comparison of the Functionality of Antibodies immobilized on Surfaces with Varying degrees of Surface Roughness”, in preparation.

Thesis

Rachel Danczyk, "Preparation, characterization, and functionality of immuno-surfaces for biosensor applications" M.S. Thesis, Purdue University, West Lafayette, IN, USA, May 2003

Tuttle,P., "Influence of biologically inspired surface roughness on antigen-antibody interactions", M.S. Thesis, Purdue University, West Lafayette, IN, USA, Dec 2004

Conference

Tuttle, P., HogenEsch, H., Rundell, A., Webster, T. “Cell Mimicked Nano-Structured Surface Roughness Membranes for Antibody-Based Biosensors”, BMES 2004.

Zheng, Y., Tuttle, P., Danczyk, R., HogenEsch, H., Webster, T., Rundell, A., “A Kinetic Analysis of the Non-Specific Interactions at Biosensor Immuno-Surfaces”, Invited presentation at BMES Oct 2003, Nashville, TN

Tuttle, P., Danczyk, R,, HogenEsch, H., Webster, T., Rundell, A., “Development of Ceramic Controlled Nano-Structured Surface Roughness for Antibody-Based Biosensors”, BMES Oct 2003, Nashville, TN

R. C. Danczyk, A. R. Baker, A. Gaba, M. R. Ladisch, T. J. Webster, A. E. Rundell “Immuno-Surface Fabrication for Biosensor Optimization”, Proceedings of the Second Joint EMBS/BMES Conference, Houston, TX, USA, pages 1714 - 1715, Oct 23-26 2002.

Y. Zheng, A. North, R. Danczyk, T. Webster, H. HogenEsch, and A. Rundell “Exploring Antigen Valency and Size Effects on Capture by Immuno-surfaces Through Analysis and Experimentation”, IEEE-EMBS Conference on Microtechnologies in Medicine and Biology, May 2002.

7.0 References

Ahluwalia, A, DeRossi, D, Ristori, C, Schirone, A, Serra, C. 1991. A Comparative Study of Protein Immobilization Techniques for Optical Immunosensors. Biosensors & Bioelectronics 7:207-214.

Alberts, B., A. Johnson, J. Lewis, M. Raff, K. Roberts, P. Walter, *Molecular Biology of the Cell*, 4th Edition, New York, NY: Garland Science, page 1375, 2002.

Anderson, GP, Jacoby, MA, Ligler, FS, King, KD. 1997. Effectiveness of Protein A for Antibody Immobilization for a Fiber Optic Biosensor. Biosensors & Bioelectronics 12(4):329-336.

Aslam, M, Dent, A. 1998. Bioconjugation: Protein Coupling Techniques for the Biomedical Sciences. New York: Grove's Dictionaries. p505-569.

Babacan, S, Pivarnik, P, Letcher, S, Rand, AG. 2000. Evaluation of Antibody Immobilization Methods for Piezoelectric Biosensor Application. Biosensors & Bioelectronics 15:615-621.

Berzofsky, J., I. Berkower, and S. Epstein, "Antigen-antibody interactions and monoclonal antibodies", (W. Paul) ed., *Fundamental Immunology*, 4th Edition, Philadelphia, PA, Lippincott-Raven Publishers, 1999.

Bhatia, SK, Teixeira, JL, Anderson, M, Shriver-Lake, LC, Calvert, JM, Georger, JH, Hickman, JJ, Dulcey, CS, Schoen, PE, Ligler, FS. 1993. Fabrication of Surfaces Resistant to Protein Adsorption and Application to Two-Dimensional Protein Patterning. Analytical Biochemistry 208:197-205.

Chen, S., L. Liu, J. Zhou, S. Jiang, "Controlling antibody orientation on charged self-assembled monolayers", Langmuir, 19, 2859-2864, 2003.

Danczyk, R. , B. Krieder, A. North, T. Webster, H. HogenEsch, and A. Rundell "Comparison of the Functionality of Antibody Immobilization Methods", Biotechnology and Bioengineering, 84:215-223, 2003.

Edwards, D., B. Goldstein, and D. Cohen, "Transport-effects on surface-volume biological reactions", *Journal of Mathematical Biology*, vol. 39, pp. 533-561, 1999.

Harlow, E., and D. Lane, *Using Antibodies: a Laboratory Manual*, Cold Spring NY, Cold Spring Harbor Laboratory Press, 1999.

Hlavacek, W., R. Posner, A. Perelson, "Steric Effects on Multivalent ligand receptor binding: exclusion of ligand sites by bound cell surface receptors", *Biophysical Journal*, vol. 76, pp. 3031-3043, 1999.

König, B, Grätzel, M. 1994. A Novel Immunosensor for Herpes Virus. Analytical Chemistry 66:341-344.

Kouvroukoglou, S, Dee, KC, Bizios, R, McIntire, LV, Zygourakis, K. 2000. Endothelial Cell Migration on Surfaces Modified with Immobilized Adhesive Peptides. Biomaterials 21:1725-1733.

Lu, B, Smyth, MR, O'Kennedy, R. 1996. Oriented Immobilization of Antibodies and Its Applications in Immunoassays and Immunosensors. Analyst 121:29R-32R.

Mason., T., A. Pineda, C. Wofsy, and B. Goldstein, "Effective rate models for the analysis of transport-dependent biosensor data", *Mathematical Biosciences*, vol. 159, pp. 123-144, 1999.

Myszka, D. , X. He, M. Dembo, T. Morton, and B. Goldstein, "Extending the range of rate constants available from BIACORE: Interpreting Mass Transport-Influenced Binding Data", *Biophyical Journal*, vol. 75, pp. 583-594, 1998.

Paek, S. and W. Schramm, "Modeling of Immunosensors under Nonequilibrium Conditions", *Analytical Biochemistry*, vol. 196, pp. 319-325, 1991.

Perelson, A., and C. DeLisi, "Receptor clustering on a cell surface. Part I. Theory of receptor cross-linking by ligands bearing two chemically identical functional groups", *Math. Biosciences*, vol. 48, pp. 71-110 1980.

Qian, W.P., et al., *Immobilization of antibodies on ultraflat polystyrene surfaces.* Clinical Chemistry, 2000. **46**(9): p. 1456-1463.

Roitt, I., J. Brostoff, D. Male, *Immunology*, Philadelphia, PA: Mosby, 3rd Edition, 1993.

Schumaker, V., M. Phillips, D. Hanson. Dynamic aspects of antibody structure, *Mol. Immunol.*, vol. 28, pp. 1347-1360, 1991.

Shriver-Lake, LC, Donner, B, Edelstein, R, Breslin, K, Bhatia, SK, Ligler, FS. 1997. Antibody Immobilization Using Heterobifunctional Crosslinkers. Biosensors & Bioelectronics 12:1101-1106.

Sulzer, B., A. Perelson, "Equilibrium Binding of Multivalent Ligands to Cells: Effects of Cell and receptor Density", *Mathematical Biosciences* vol. 135, pp. 147-185, 1996.

Paul Tuttle, "Influence of biologically inspired surface roughness on antigen-antibody interactions", M.S. Thesis, Purdue University, West Lafayette, IN, USA, Dec 2004

Turkova, J. 1999. Oriented Immobilization of Biologically Active Proteins as a Tool for Revealing Protein Interactions and Function. Journal of Chromatography B 722:11-31.

Vijayendran, R., F. Ligler, and D. Leckband, "A computational reaction-diffusion model for the analysis of transport –limited kinetics", *Analytical Chemistry*, vol. 71, pp. 5405-5412, 1999.

Wade, R., J. Taveau, J. Lamy, Concerning the axial flexibility of the Fab regions of immunoglobulin G., *J. Mol. Bi*ol., vol. 206, pp. 349-356, 1989.

Webster, T., "Nanophase ceramics: The future orthopedic and dental implant material," in Advances in Chemical Engineering Vol. 27 (J. Ying, editor), pp. 125-166, NY, Academic Press, 2001.

Weimer, B., M.Walsh, X. Wang, "Influence of a poly-ethylene glycol spacer on antigen capture by immobilized antibodies", *J. Biochem. Biophys. Methods*, vol. 45, pp. 211-219, 2000.

Ying, J.Y.-R., *Nanostructured materials*. 2001, San Diego: Academic. xii, 222.

Zull, JE, Reed-Mundell, J, Lee, YW, Vezenov, D, Ziats, NP, Anderson, JM, Sukenik, CN. 1994. Problems and Approaches in Covalent Attachment of Peptides and Proteins to Inorganic Surfaces for Biosensor Applications. Journal Industrial Microbiology 13:137-143.

Appendix A: Parameter Definitions and Values

Description	Parameter Variable	value or calculation	units
Antigen Parameters			
Epitope density on antigen	ρ	1e15	#/dm^2
Diameter of antigen	D	5e-6	dm
# of epitopes per antigen	N	$round(P \times \pi D^2)$	#
Antigen concentration	x_0	7.55e-8	M
Antigen Contact Area	A	$\frac{\pi D^2 L}{D + 2L}$	dm^2
Antibody Contact Area	A_s	$\pi(DL + L^2)$	dm^2
# of epitopes in the antigen contact area A	n	$round(P \times A)$	#
Antibody Parameters			
Blocked area on antigen by an antibody	a	2.54e-14	dm^2
Antibody contact area on antigen epitope	a_p	2e-15	dm^2
Antibody length	$\bar{L}$	1.1e-7	dm
Antibody density	R_I	6.5e-12	mole/ dm^2
# of antibodies in the antibody contact area As	f	$\text{round}(Na \times R_I \times A_s)$	#
Antibody flexibility on the surface	γ	1	100%
Kinetic rate parameters			
Initial association rate	k_1	4.1e5/N	dm^2/(mole sec)
Initial dissociation rate	k_{-1}	0.1	s^{-1}
Crosslinking forward rate	k_x	4.1e7	dm^2/(mole sec)
Crosslinking reverse rate	k_{-x}	0.1	s^{-1}
Chamber coefficients			
Immuno-surface area	S	1	dm^2
Volume of the chamber	V1	1	dm^3
Simulation duration			
Duration of association phase	T1	100	sec
Duration of dissociation phase	T2	100	sec

List of Abbreviations

AFM	Atomic Force Microscope
ANOVA	Analysis of Variance
BMPS	N-Maleoyl-ß-alanine N-hydroxysuccinimide ester
BCR	B Cell Receptor
BSA	Bovine Serum Albumin
DNP	2,4dinitrophenol
EDC	1-Ethyl-3-(3-dimethylaminopropyl)carbodiimide
EMCS	N-(6-Maleimidocaproyloxy)succinimide
Fab	Antigen binding fragment of an antibody
Fc	Non-antigen binding fragment of an antibody (separated from the Fab by pepsin)
GMBS	N-(4-Maleimidobutyryloxy)succinimideN-Succinimidyl-4-maleimidobutyrate
IgG	Immunoglobulin G
MS	Microspheres
MW	Molecular Weight
PA	Protein A
PBS	Phosphate Buffered Saline
PEG	Polyethylene Glycol
RMS	Root-Mean-Square
SAC	Specific Antigen Capture
SEM (p7)	Standard error of the mean